Guide to Design with Fiber-Reinforced Concrete

Reported by ACI Committee 544

ACI 544.4R-18

American Concrete Institute
Always advancing

First Printing
July 2018
ISBN: 978-1-64195-019-0

Guide to Design with Fiber-Reinforced Concrete

Order information: ACI documents are available in print, by download, through electronic subscription, or reprint and may be obtained by contacting ACI.

Most ACI standards and committee reports are gathered together in the annually revised the ACI Collection of Concrete Codes, Specifications, and Practices.

American Concrete Institute
38800 Country Club Drive
Farmington Hills, MI 48331
Phone: +1.248.848.3700
Fax: +1.248.848.3701

www.concrete.org

ACI 544.4R-18

Guide to Design with Fiber-Reinforced Concrete

Reported by ACI Committee 544

Barzin Mobasher*, Chair
Neven Krstulovic-Opara, Secretary

Clifford N. MacDonald, Membership Secretary

Corina-Maria Aldea
Salah Ahmed Altoubat*
Emmanuel K. Attiogbe*
Mehdi Bakhshi*
Nemkumar Banthia
Joaquim Oliveira Barros*
Amir Bonakdar*†
Amanda C. Bordelon
Jean-Philippe Charron
Xavier Destree*

Ashish Dubey
Mahmut Ekenel
Alessandro P. Fantilli
Liberato Ferrara*
Gregor D. Fischer
Dean P. Forgeron
Emilio Garcia Taengua*
Rishi Gupta
Marco Invernizzi
John Jones

David A. Lange
Michael A. Mahoney*
Bruno Massicotte*
James Milligan
Nicholas C. Mitchell Jr.
Verya Nasri
Jeffrey L. Novak*
Giovanni A. Plizzari*
Klaus Alexander Rieder*
Pierre Rossi

Steve Schaef*
Surendra P. Shah
Flavio de Andrade Silva
Luca Sorelli
Gerhard Vitt*
Thomas E. West Jr.
Kay Wille
Robert C. Zellers

Consulting Members

P. N. Balaguru
Hiram Price Ball Jr.
Gordon B. Batson

Arnon Bentur
Andrzej M. Brandt
James I. Daniel

Sidney Freedman
Christian Meyer
Antoine E. Naaman*

Venkataswamy Ramakrishnan

*Members of the task group that prepared this guide.
†Chair of the task group that prepared this guide.

The committee would like to thank the following for their contribution to this guide: A. Burran, H. Helmink, and A. Lubell.

New developments in materials technology and the addition of field experience to the engineering knowledge base have expanded the applications of fiber-reinforced concrete (FRC). Fibers are made with different materials and can provide different levels of tensile/flexural capacity for a concrete section, depending on the type, dosage, and geometry. This guide provides practicing engineers with simple, yet appropriate, design guidelines for FRC in structural and nonstructural applications. Standard tests are used for characterizing the performance of FRC and the results are used for design purposes, including flexure, shear, and crack-width control. Specific applications of fiber reinforcement have been discussed in this document, including slabs-on-ground, composite slabs-on-metal decks, pile-supported ground slabs, precast units, shotcrete, and hybrid reinforcement (reinforcing bar plus fibers).

Keywords: crack control; fiber-reinforced concrete; flexural toughness; macrofiber; moment capacity; precast; residual strength; shear capacity; shotcrete; slabs-on-ground; steel fibers; synthetic fibers; tensile strength; toughness.

CONTENTS

CHAPTER 1—INTRODUCTION AND SCOPE, p. 2
1.1—Introduction, p. 2
1.2—Scope, p. 3
1.3—Historical aspects, p. 3

CHAPTER 2—NOTATION AND DEFINITIONS, p. 6
2.1—Notation, p. 6
2.2—Definitions, p. 7

CHAPTER 3—CHARACTERISTICS OF FRC, p. 7
3.1—Classification of fibers, p. 7
3.2—Performance of FRC, p. 8
3.3—Standard test methods for FRC, p. 9
3.4—Strain softening and strain hardening, p. 10

ACI 544.4R-18 supersedes ACI 544.4R-88 and was adopted and published July 2018.

CHAPTER 4—DESIGN CONCEPTS AND GUIDES, p. 13

4.1—Design concepts, p. 13

4.2—Tensile stress-strain response for FRC, p. 13

4.3—Correlation of tensile and flexural response for FRC, p. 13

4.4—Design of RC for flexure (stress block), p. 14

4.5—Design of FRC for flexure (ASTM C1609/C1609M, in conjunction with RILEM TC 162-TDF [2003]), p. 14

4.6—Design of FRC for flexure (Model Code 2010 [*fib* 2013]), p. 15

4.7—Design of FRC for flexure-hybrid reinforcement, p. 16

4.8—Design of FRC for shear, p. 17

4.9—Parametric-based design for FRC, p. 18

CHAPTER 5—DESIGN FOR SPECIFIC APPLICATIONS, p. 21

5.1—Slabs-on-ground, p. 21

5.2—Extended joint spacing, p. 23

5.3—Elevated floors/slabs-on-piles, p. 24

5.4—Composite steel decks, p. 24

5.5—Precast units, p. 25

5.6—Shotcrete, p. 26

5.7—Crack control and durability, p. 27

CHAPTER 6—CONSTRUCTION PRACTICES, p. 28

6.1—Mixture design recommendations for FRC, p. 28

6.2—Workability of FRC, p. 28

6.3—Adding and mixing fibers, p. 28

6.4—Placing, consolidation, and finishing FRC, p. 28

6.5—Quality control for FRC, p. 30

6.6—Contraction (control) joints, p. 30

6.7—Specifying FRC, p. 30

CHAPTER 7—REFERENCES, p. 30

Authored references, p. 31

APPENDIX—SOLVED EXAMPLE PROBLEMS FOR SECTION 4.9—PARAMETRIC BASED DESIGN FOR FRC, p. 34

Case A: Calculation of the moment capacity of a given section, p. 34

Case B: Calculation of μ based on parametric-based design for FRC (ACI 544.8R), p. 36

Case C: Calculation of μ for the replacement of reinforcement in a singly reinforced slab (ACI 544.8R), p. 37

CHAPTER 1—INTRODUCTION AND SCOPE

1.1—Introduction

The aim of this guide is to provide practicing engineers with design guidelines and recommendations for fiber reinforcement. Several approaches for designing fiber-reinforced concrete (FRC) have been developed over the years that are based on conventional design methods modified by special procedures to account for contributions of the fibers. These methods generally modify the internal forces in the member to account for the additional tensile capacity provided by the fibers. When compared with full-scale test data, these methods have provided satisfactory designs for FRC members (Parra-Montesinos 2006; Moccichino et al. 2006; Altoubat et al. 2009).

Concrete is a brittle material that is strong in compression but weak in tension. Steel bars are traditionally used to carry the tensile forces after concrete has cracked in structural applications. In reinforced concrete, the tensile strain of the concrete at cracking is much lower than the yield strain of the steel bars, which results in cracking of concrete before any significant load is transferred to the steel. Steel reinforcement is also used to limit the crack widths under specified levels for serviceability requirements. Unlike reinforcing bars, fibers are uniformly distributed in the volume of concrete; hence, the distance between fibers is much smaller than the spacing between bars. Fibers can provide post-crack tensile and flexural capacity and crack-width control in concrete elements.

Natural sources of reinforcement were used for brittle construction materials more than 3000 years ago, such as straw reinforcement in mud bricks. The first scientific studies on the use of steel fibers in concrete date back to the 1960s (Romualdi and Batson 1963; Naaman and Shah 1976). Since then, thousands of projects have been successfully completed using fiber reinforcement, including slabs-on-ground, composite steel decks, slabs-on-pile, precast, and shotcrete.

The major differences in the proposed methods are in the determination of the increase in tensile capacity of concrete provided by the fibers and the manner in which the total force is calculated. A conservative but justifiable approach in structural members such as beams, columns, walls, or elevated suspended slabs is that reinforcing bars should be used to support the total tensile loads. ACI 544.6R, however, describes the design for elevated suspended slabs where steel fibers are used as the primary reinforcement along with a minimum of continuous bars from columns to columns. Fibers can be used, in general, to supplement and reduce the reinforcing bars in various structural members. In applications where the presence of continuous reinforcement is not essential to the safety and integrity of the structure such as slabs-on-ground, pavements, overlays, shotcrete linings, slabs-on-piles (ACI 544.6R), and some precast units, fibers may be used as the sole means of reinforcement.

Fibers reliably control cracking and improve material resistance to deterioration as a result of fatigue, impact, and shrinkage, or thermal stresses. Fibers can contribute to the improved performance of concrete members in two ways: 1) by resisting the tensile stresses and, therefore, playing a structural role; or 2) by controlling crack development and, therefore, improving the durability of concrete. When fibers are intended to contribute to the structural performance of an element or structure, the FRC should be designed accordingly and the fiber contribution to the load-bearing capacity should be properly assessed and justified.

The commercial momentum for using steel fibers occurred during the 1970s for industrial floors as a major application. Other applications for steel fibers include composite metal deck, pile-supported slabs, precast units, and shotcrete. Synthetic macrofibers became available in the 1990s with applications such as slabs-on-ground, composite decks, pavements, shotcrete, and some precast units. Steel fibers and synthetic macrofibers can be viable alternatives for full replacement of steel bars in concrete elements with continuous support such as slabs-on-ground or shotcrete. For free-standing elements such as suspended slabs and tunnel lining segments, steel fibers at medium to high dosages have been shown to successfully replace a large portion of steel bars in the section (ACI 544.6R; ACI 544.7R).

The term "fibers" in this document only concerns macrofibers made of steel and polymeric (polyolefin) synthetic materials; hence, the design guides are not applicable to microfibers. Fiber diameter of 0.012 in. (0.3 mm) is the defining limit between microfibers and macrofibers. Synthetic microfibers have been used in concrete since the 1970s and are solely intended to control plastic shrinkage cracks (and sometimes drying shrinkage cracks) without any significant improvement in the mechanical properties of hardened concrete (ACI 360R). They may also affect the bleeding rate of fresh concrete, improving the near-surface properties of the hardened concrete. These fibers have been used to reduce the spalling of concrete exposed to fire and explosion.

When macrofibers are used in concrete to replace steel reinforcement, they can provide enhanced ductility, toughness, and durability. Fiber dosage can be engineered to provide a desired level of crack control, post-crack tensile and flexural capacity, or both. Similar to steel bars for which the size and spacing are calculated to provide the required reinforcement ratio, the dosage of fibers is also calculated to satisfy engineering requirements. Parameters affecting the performance of FRC include fiber type (material, size, and geometry), as well as bond characteristics and concrete mixture design. Fiber dosage may be limited by the practicality of their use in concrete; however, chemical admixtures are widely used for incorporating higher dosages of fibers. In certain applications, especially with congested steel bars, hybrid reinforcement (steel bars plus fibers) can be a viable alternative to conventional reinforcement. Using FRC may allow for applying alternative construction techniques—for example, tailgating concrete instead of pumping it for slabs-on-ground when steel reinforcement is eliminated. This can help in scheduling the project, resulting in a more cost-effective construction. Improved job-site safety is also among the benefits of using fibers from the reduced handling or tripping over the reinforcement at the job site. Using fibers can additionally eliminate the problems caused by misplacing conventional steel at its design position. The durability aspects of FRC and the associated benefits from fibers are extensively presented in ACI 544.5R.

1.2—Scope

Although FRC has been used since the 1960s, there are no agreed design approaches in North America for some of its applications. Unlike reinforced concrete with steel bars or welded wire mesh, the design of fiber reinforcement is not properly covered by national design codes. In Model Code 2010 (*fib* 2013), sections were added for new developments in the design of FRC as a part of the building code. ACI 318 has limited discussion on the use of fibers, such as provisions for using steel fibers as shear reinforcement in flexural members. ACI 360R presents the basics of fiber-reinforced slabs-on-ground, and ACI 506.1R discusses the design and application of fiber-reinforced shotcrete. It is the intent of this document to provide practicing engineers with simple yet appropriate design guidelines and state-of-the-art applications for FRC. This guide is intended for designers who are familiar with structural concrete containing conventional steel reinforcement, but who may need more guidance on the design and specification for FRC. In this document, fibers are treated as reinforcement in concrete and not as an admixture.

This guide discusses the types and typical dosages for fibers, general material properties, and available test methods for characterization of FRC. Explaining the design concepts and existing guidelines for fiber reinforcement is the focus of this document, including constitutive laws, design for flexure, design for shear, and design for crack-width control. This is further extended to specific applications for slabs-on-ground, composite slabs-on-metal decks, pile-supported ground slabs, precast units, shotcrete, and special applications. The final portion of this guide provides brief recommendations for specifying and building with FRC that includes general guidelines for mixing, placing, and finishing.

Although there are several types of fibers commercially available, this document is only applicable to steel fibers and polyolefin synthetic macrofibers that comply with ASTM C1116/C1116M. The formulas and applications discussed in this document should be verified for any other types of fibers. This document provides design guidelines based on the mechanical and structural properties of FRC as a composite material and not individual fiber products. Different fiber products may exhibit different performances in concrete; hence, it is crucial to design and specify FRC properties in addition to fiber types and materials that are suitable to achieve such properties.

1.3—Historical aspects

1.3.1 *Introduction*—Prior to presenting test methods, design philosophies, and applications of FRC, it is beneficial to review some of the historical aspects of this technology. This section summarizes the historical background of FRC since its development, including the mechanical characterization, analytical modeling, and test methods. Some of the earlier design and analysis guides addressing FRC during the 1970s and 1980s are discussed in Hoff (1982), ACI SP-44, SP-81, SP-105, and Shah and Skarendahl (1986). It should be noted that most of the earlier studies and applications of FRC incorporated steel fibers only.

1.3.2 *Mechanical characteristics and modeling*—Understanding the mechanical properties of FRC and their variation with fiber type and dosage is an important aspect of successful design. Fibers influence the mechanical properties of concrete in all failure modes, including compression, tension, bending, shear, impact, and fatigue (Gopalaratnam and Shah 1987a). Excluding plain matrix properties, the most important variables governing the properties of FRC are the fiber bond efficiency and dosage. Fiber bond efficiency is controlled by the resistance of the fibers to pullout, which in turn depends on the bond strength at the fiber-matrix interface. Certain types of fibers may go through elongation and eventual rupture during the energy-absorbing process.

Pullout-type mechanisms are gradual and ductile compared with the more rapid and possibly tensile failure of fibers in tension. An alternative mechanism is provided by fibers whose anchoring system prevents pullout and provides ductility through the elongation of the fiber itself. The strengthening mechanism of the fibers involves transfer of stress from the matrix to the fiber by interfacial shear or by interlock between the fiber and matrix if the fiber surface is deformed. Stress is thus shared by the fiber and matrix in tension until the matrix cracks and then the total stress is progressively transferred to the fibers (Naaman and Shah 1976). The crack control through pullout-resisting mechanisms that is achieved from fibers bridging the crack surfaces will result in an increase in the load-carrying capacity, the energy dissipation (ductility), and at ultimate limit design states for FRC (Cunha 2010). Several models in a design practice format, such as closed-form solutions, have been proposed (Stang and Olesen 1998; Olesen 2001). More recently, Soranakom and Mobasher (2007) developed a closed-form solution capable of determining the moment-curvature relationship of a cross section of a beam reinforced longitudinally with steel bars and made with FRC. With the advent of new generations of fibers and chemical admixtures, as well as enhanced knowledge of particle distribution process, behavior of aggregate-paste and fiber-paste interface zones, specialty FRC mixtures have been developed. The special characteristics for these materials include post-crack tensile strength that is higher than the material strength at crack initiation (Fantilli et al. 2009).

1.3.3 *Compression*—At typical dosages, the effect of fibers on the compressive strength of concrete has been shown to be marginal to negligible (Shah et al. 1978; Fanella and Naaman 1985). Documented increases in compressive strength range from negligible in most cases to 23 percent for concrete containing 2 percent by volume of steel fiber (equal to 266 lb/yd^3 [160 kg/m^3]) with an aspect ratio of 100, tested with 6 x 12 in. (150 x 300 mm) cylinders (Williamson 1974). More recently, higher values of post-crack compressive strength have been reported using new generation of steel fibers (El-Dieb 2009).

Typical stress-strain curves for steel FRC in compression, at higher dosages, show a substantial increase in the strain at the peak stress and the slope of the descending portion is less steep than that of control specimens without fibers (Fanella and Naaman 1985). This is indicative of substantially higher toughness as a measure of the ability to absorb energy during deformation. The improved toughness in compression imparted by fibers is useful in preventing sudden and explosive failure under static loading, and in absorbing energy under dynamic loading. It should be noted that the modulus of elasticity of concrete (in the linear ascending precrack region) is not affected by the fibers because they are only effective after concrete has cracked. During the failure stage in compression (after cracking), fibers guarantee a passive confinement similar to that of transverse reinforcement (Fantilli et al. 2011a,b). As a result, in reinforced concrete columns made with high-strength mixtures, the presence of fibers prevents the premature spalling of the brittle concrete cover and improves the ductility of the axially loaded members (Paultre et al. 2010).

1.3.4 *Direct tension*—Experimental procedures for measuring the tensile stress-strain curves for steel FRC date back to the work of Shah et al. (1978) and Gopalaratnam and Shah (1987b). Standardized direct tension tests for concrete are not available because of the variations in testing, which is attributed to the size of the specimen, concrete crushing at grips, stiffness of the testing machine, gauge length, mode of test control (closed loop versus open loop), and whether single or multiple cracks are present. While the initial ascending part of the curve up to first-cracking is similar to that of unreinforced concrete, strain-softening or strain-hardening behaviors can be observed in different specimens. The descending part depends on the stress-crack width relationship and fiber parameters such as geometry, material, dosage, and aspect ratio (Visalvanich and Naaman 1983). If only a single crack forms in the tension specimen, deformation is concentrated at the crack and the calculated strain depends on the gauge length. Thus, post-crack strain information should be interpreted with care in the post-crack region. The strength of FRC in direct tension (before cracking) is generally of the same order as that of unreinforced concrete—that is, 300 to 900 psi (2 to 6 MPa). Its toughness can be two to three orders of magnitude higher, primarily because of the energy absorption during fiber pullout and the deformation of multiple cracks (Shah et al. 1978; Visalvanich and Naaman 1983; Gopalaratnam and Shah 1987b). Many direct and indirect procedures have been developed for stress-crack width relationship measurement in FRC using direct tension test or a flexural test (Vandewalle 2000a,b, 2002). Details on such calculations can be found in ACI 544.8R.

1.3.5 *Flexural strength*—The influence of fibers on flexural response of concrete is much greater than on compressive response. Two flexural strength values are commonly reported. One, termed the first-peak strength (first-crack flexural strength), corresponds to the load at which the load-deformation curve departs from linearity. This is when concrete matrix cracks. The other corresponds to the maximum load achieved, commonly called the ultimate flexural strength, peak strength, or modulus of rupture. Strengths are calculated from the corresponding load using the formulas for modulus of rupture given in ASTM C78/C78M, although the linear stress and strain distributions on which the formula is based no longer apply after the matrix has cracked. Procedures for determining first-crack and ultimate flexural strengths, as discussed in ACI 544.2R and ASTM C1609/C1609M, are based on testing 6 x 6 x 20 in. (150 x 150 x 500 mm) beams using four-point loading configuration as well as BS EN 14651:2005 using 6 x 6 x 22 in. (150 x 150 x 550 mm) beams with a notch at midspan and three-point loading. Other sizes and shapes may provide higher or lower strengths, depending on span length, width, and depth of cross section, and the ratio of fiber length to the minimum cross-sectional dimension of the test specimen.

The original approach of predicting the flexural strength of small beams reinforced with steel fibers was done by Swamy et al. (1974), who used empirical data from laboratory experiments, using the fiber bond and introduced a random distribution factor, bond stress, and fiber stress. Based on the ACI 318 ultimate strength design method, the tensile strength of the fibrous concrete is added to the contribution by the reinforcing bars to obtain the ultimate moment (Henager and Doherty 1976).

1.3.6 *Toughness and residual strength*—Toughness is one of the most important characteristics of FRC. Flexural toughness may be defined as the area under the load-versus-deflection (or load versus crack opening) curve in a beam test, which is the total energy absorbed prior to complete failure of the specimen. Flexural toughness indexes were used in the past as the ratio of the area under the load-deflection curve for FRC to a specified point, to the area up to first crack (Bonakdar et al. 2005). In more recent years, the parameter residual strength has replaced the toughness index for characterizing FRC. The strength of FRC after concrete has cracked is referred to as residual strength, typically expressed in psi or MPa. The residual strength can be measured in flexure or tension, depending on the test; however, the term "residual strength" is typically for flexure, obtained from a beam test such as ASTM C1609/C1609M and BS EN 14651:2005. Round panels have also been used according to ASTM C1550, specifically for measuring the flexural toughness or energy absorption of fiber-reinforced shotcrete; this parameter is typically expressed in joules. These panels are 32 in. (800 mm) in diameter and approximately 3 in. (75 mm) in thickness and are tested using three supports and one central loading point.

FRC is superior to plain concrete in fracture energy. Whereas the traditional fracture mechanics are used to quantify the energy to initial cracking in the material, the total fracture energy parameter originally suggested by Hillerborg (1985) quantifies the energy to propagate the crack to complete failure. Although there is no standard test for quantifying fracture of concrete and FRC, several recommended test procedures have been implemented. Test results for total fracture energy of FRC can vary due to the heterogeneous nature of the material. More details on the test methods and quantification of FRC for total fracture energy have been published by Kim and Bordelon (2015) and Mobasher et al. (2015a).

1.3.7 *Shear*—Use of fibers as shear reinforcement in reinforced concrete beams has been the focus of several investigations in the past four decades (Mansur et al. 1986; Kwak et al. 2002; Minelli and Vecchio 2006; Parra-Montesinos 2006; Altoubat et al. 2009; Shoaib et al. 2014). Research by Talboys and Lubell (2014) has demonstrated that the shear stress at failure in steel FRC beams and slabs decreases as the strain in the longitudinal reinforcing bars increases. This can be explained by the fact that fiber reinforcement enhances shear resistance of concrete by bridging tensile stresses across diagonal cracks. This can result in a reduction of diagonal crack spacing and width, which improves aggregate interlock effects. The reduction in crack spacing due to the presence of fibers indicates that the use of fibers could lead to a reduction of the size effect in shear for beams and slabs without stirrups where the shear at failure is known to decrease as the overall beam depth increases. ACI 318-14 Section R26.12.5 briefly presents the performance criteria for using steel fibers as shear reinforcement in structural elements.

Numerous tests indicate that stirrups and fibers can be used effectively in combination (Altoubat et al. 2009). The increase in shear capacity due to fiber reinforcement has been quantified in several investigations and steel fibers have been used in practical applications to replace the stirrups. More recently, both steel and synthetic macrofibers have been employed in concrete for full-scale tests in flexural members (Altoubat et al. 2009; Minelli et al. 2014; Shoaib et al. 2014; Conforti et al. 2015).

Earlier studies conducted include the work of Batson et al. (1972) with steel fibers, in which tests on 96 beams were performed varying the fiber size, type, and volume fractions, along with the shear span-depth ratio (a/d), where a is the shear span (distance between concentrated load and face of support), and d is the depth to centroid of reinforcing bars. In third-point loading experiments, a decrease in a/d and an increase in the steel fiber volume increased the shear stresses developed at failure. A fiber volume fraction in the range of 0.88 to 1.76 percent (equal to 117 to 232 lb/yd^3 [70 to 140 kg/m^3]) for a/d = 3.6 to 2.8 would change the shear strength from 450 to 510 psi (3.1 to 3.8 MPa) and mode of failure from shear to flexure.

The earliest work addressing underground applications was by Paul and Sinnamon (1975), who used Batson's approach to determine a procedure for predicting the shear capacity of segmented concrete tunnel liners made with steel FRC (SFRC). The influence of steel fiber reinforcement on the shear strength of reinforced concrete flat plates was investigated by Swamy et al. (1979) with fiber contents of 0.6, 0.9, and 1.2 percent by volume (equal to 80, 120, and 160 lb/yd^3 [48, 72, and 96 kg/m^3]). The increase in shear strength was 22, 35, and 42 percent, respectively, compared to the control specimens.

The use of synthetic macrofibers as a means of shear reinforcement has been studied by Altoubat et al. (2009) and Yazdanbakhsh et al. (2015). Full-scale FRC beams with shear span-depth ratios of 3.5 and 2.3 were tested, and synthetic macrofibers were added at various dosages of 0.5, 0.75, and 1.0 percent volume fraction (equal to 7.5, 11.2, and 15 lb/yd^3 [4.5, 6.7, and 9 kg/m^3]). The results showed that the shear strength of the beams was increased by up to 30 percent relative to the control beam. It was shown that these fibers could provide the required shear capacity based on ACI 318, although the practical applications of synthetic fibers and code implementations have yet to be established.

1.3.8 *Shrinkage*—When concrete is tested for free shrinkage, fibers are not expected to have an effect in the absolute shrinkage value. For restrained shrinkage, however, fibers provide a means of crack control both in plastic and drying shrinkage. Tests using ring-type concrete specimens cast around a restraining steel ring, or with a stress riser, have shown that fibers can substantially reduce the amount of cracking and the mean crack width (Malmberg and Skarendahl 1978; Swamy and Stavrides 1979). Fibers can also provide an adequate internal restraining mechanism in conjunction with shrinkage-compensating cements, so that the concrete system will perform its crack control function even when restraint from conventional reinforcement is not provided. Fibers and shrinkage-compensating cements have been used in a complementary fashion by Paul et al. (1981) (refer also to ACI 223R).

CHAPTER 2—NOTATION AND DEFINITIONS

2.1—Notation

A_s = cross sectional area of steel, in.^{2} (mm^2)
a = depth of compressive zone, in. (mm)
a_e = radius of circle with area equal to that of the contact area, in. (mm)
b = section width, in. (mm)
C = equivalent compressive forces on a cross section, lbf (kN)
d = depth of reinforcement, in. (mm)
d_e = effective depth of cross section, in. (mm)
E = elastic modulus of concrete, psi (MPa)
F = force component in stress diagram, lbf (N)
$F_{Fts\text{-}FRC}$ = FRC tensile strength under serviceability state, psi (MPa)
$F_{Ftu\text{-}FRC}$ = FRC tensile strength under ultimate state, psi (MPa)
F_{st} = steel bar/mesh tensile force, lbf (N)
f_c = compressive strength of plain concrete, psi (MPa)
f_c' = specified compressive strength of concrete, psi (MPa)
f_{150}^D = FRC flexural residual strength at a deflection of L/150, psi (MPa)
f_{600}^D = FRC flexural residual strength at a deflection of L/600, psi (MPa)
$f_{e,3}$ = FRC equivalent flexural strength at a deflection of L/150, psi (MPa)
f_P = peak strength, psi (MPa)
$f_{R,1}$ = FRC flexural residual strength at CMOD$_1$, psi (MPa)
$f_{R,3}$ = FRC flexural residual strength at CMOD$_1$, psi (MPa)
f_t = tensile strength of plain concrete, psi (MPa)
$f_{ut\text{-}FRC}$ = FRC ultimate tensile residual strength, psi (MPa)
f_y = specified yield strength of steel, psi (MPa)
h = section thickness or height, in. (mm)
K = modulus of subgrade reaction, lb/in.^{3} (N/mm^3)
k = neutral axis depth ratio
k_s = factor for size effect in shear calculations
L = radius of relative stiffness, in. (mm)
M_0 = moment capacity of the slab after cracking, lb-in. (N-mm)
M_{cr} = cracking moment of a concrete section, lb-in. (N-mm)
M_n = nominal moment of a concrete or RC/FRC section, lb-in. (N-mm)
M_u = normalized ultimate moment of a section, lb-in. (N-mm)
M_u' = normalized allowable moment of a section, lb-in. (N-mm)
P_0 = known load value, lbf (kN)
P_{150}^D = FRC flexural residual load at a deflection of L/150, lbf (kN)
P_{600}^D = FRC flexural residual load at a deflection of L/600, lbf (kN)
P_P = peak load, lbf (kN)
$R_{T,150}^D$ = equivalent flexural strength ratio at a deflection of L/150, percent
T = concentrated tensile forces on a cross section, lbf (kN)
T_{150}^D = FRC flexural toughness up to a deflection of L/150, lb-in. (Joule)
w = crack width in RC/FRC section, in. (mm)
α = normalized transitional strain
β_{tu} = normalized tensile strain at maximum stress
ε_1 = tensile strain at onset of first cracking
ε_2 = tensile strain at the onset of the stable strain softening branch
ε_3 = tensile strain at the end of the softening branch
ε_c = compressive strain
ε_{cr} = first cracking tensile strain
ε_{cu} = ultimate (maximum) compressive strain
ε_{cy} = compressive strain at yielding
ε_t = tensile strain
ε_{tu} = ultimate (maximum) tensile strain
γ_c = partial safety factor for plain concrete
λ = normalized top compressive strain
λ_{cu} = normalized ultimate (maximum) compressive strain
λ_{tu} = normalized compressive strain when reaching ultimate tensile strain
μ = normalized post-peak residual tensile strength
μ_{crit} = critical normalized post-peak residual tensile strength
ν = concrete Poisson's ratio
ρ = reinforcement ratio for longitudianl reinforcement, $\rho = A_s/(bd)$
σ_1 = tensile stress at onset of first cracking, psi (MPa)
σ_2 = tensile stress at the onset of the stable strain softening branch, psi (MPa)
σ_3 = tensile stress at the end of the softening branch, psi (MPa)
σ_c = compressive stress, psi (MPa)
σ_{cp} = average normal stress acting on concrete cross section, psi (MPa)
σ_{cy} = compressive yield strength, psi (MPa)
σ_p = post-crack tensile strength, psi (MPa)
σ_t = tensile stress, psi (MPa)
φ = curvature, 1/in. (1/mm)
φ_{cr} = cracking tensile strength, psi (MPa)
φ_u = maximum curvature, 1/in. (1/mm)
ω = compressive to tensile strength ratio

2.2—Definitions

Please refer to the latest version of ACI Concrete Terminology for a comprehensive list of definitions. Definitions provided herein complement that resource.

aspect ratio—ratio of the length to the diameter or the equivalent diameter of one single fiber.

balling—formation of large clumps of entangled fibers that may occur before or during the mixing process.

chemical bond fibers—fibers whose composition or surface characteristics promote chemical interaction with the concrete matrix to increase bond strength.

collated fibers—fibers bundled together either by cross-linking or by chemical or mechanical means.

denier—a number equivalent to the mass in grams of 9000 meters of a continuous fiber filament.

ductility—the ability of a material to undergo permanent deformation without rupture.

embossed fibers—fibers with surface indentations or ripples that provide mechanical anchorage with the concrete matrix.

equivalent diameter of fiber—diameter of a circle with an area equal to the average cross-sectional area of the fiber.

equivalent flexural residual strength—average flexural stress measured for a fiber-reinforced concrete beam, up to a specified deflection or crack width.

equivalent flexural residual strength ratio—ratio of the equivalent flexural residual strength and the flexural strength of concrete, percent.

fiber dosage—total fiber mass or weight in a unit volume of concrete, generally expressed in lb/yd^3 (kg/m^3).

fiber volume fraction—total fiber volume in a unit volume of concrete (generally expressed as a percentage).

fibrillated fibers—fiber configuration that has sections of the fiber splitting to form fiber branches (before mixing into concrete).

fibrillating fibers—fiber configuration that has sections of the fiber splitting to form fiber branches (after mixing into concrete).

limit of proportionality—flexural stress measured at the onset of first cracking in a bending test.

monofilament fibers—single fiber, which may be circular or prismatic in cross section.

residual flexural strength—flexural strength retained in a cracked FRC beam, measured at a certain deflection or crack width.

steel fibers—discrete fibers made of steel, used as reinforcement in concrete.

synthetic fibers—chopped fibers made of polyolefin, such as polypropylene and polyethylene materials, used as reinforcement in concrete.

CHAPTER 3—CHARACTERISTICS OF FRC

3.1—Classification of fibers

Fibers come in different material types, geometries, and sizes and typically range from 1/8 to 2.5 in. (3 to 65 mm) in length. ASTM C1116/C1116M classifies FRC based on the fiber material. These fibers include steel, glass, synthetic, and natural. A subclassification is often used based on the size and functionality of the fibers; hence, fibers can be classified as microfibers or macrofibers with the fiber diameter of 0.012 in. (0.3 mm) as the separating limit. On a much smaller scale, nanofibers also exist whose contribution to concrete properties are quite different than microfibers and macrofibers, and are not discussed herein. Steel fibers and polymeric synthetic fibers are the most-used types of fibers in construction industry and are the focus of this document. Other types of synthetic fibers, such as PVA and glass, have been used in some limited applications for concrete reinforcement; however, they are outside the scope of this document. The design guidelines in this guide have been derived and verified for FRC with steel and synthetic macrofibers only. Therefore, they should not be applied to any other types of FRC without a detailed evaluation and proof of the applicability.

3.1.1 *Steel fibers*—ASTM A820/A820M is the standard specification for steel fibers for use in concrete. Steel fibers for concrete reinforcement are short, discrete lengths of steel sufficiently small to be randomly dispersed in concrete using common mixing procedures. ASTM A820/A820M provides classification for five general types of steel fibers, based primarily on the product or process used in their manufacture: Type I: cold-drawn wire; Type II: cut sheet; Type III: melt-extracted; Type IV: mill cut; and Type V: modified cold-drawn wire. Steel fibers come in many geometries, including rectangular, flat, cylindrical, and variations or combinations of these. In addition, fiber anchorage mechanisms in concrete include continuous deformations such as twists, dimples or crimps, end anchorage such as hooks, or simply bond for undeformed fibers. Bond to the concrete matrix is enhanced by mechanical anchorage, surface area, alloying, surface roughness, or a combination of these. Fiber geometry and anchorage significantly affects resistance to pullout forces and overall performance of FRC. Another characteristic is the aspect ratio or the ratio of the length to diameter. Typically, for the same mixture proportions, as the fiber aspect ratio increases, so does the reinforcing performance. According to ASTM A820/A820M, the average tensile strength of fiber material should not be less than 50,000 psi (345 MPa). Steel macrofibers have typical diameters in the range of 0.01 to 0.05 in. (0.3 to 1.3 mm) and a length in the range of 1.2 to 2.5 in. (30 to 65 mm). The actual dosage for steel fibers depends on the specific application and the required engineering performance, as described in later chapters. Specifications should include the performance requirements rather than the prescriptive dosage for fibers.

3.1.2 *Synthetic fibers*—Synthetic fibers are made with polyolefin materials, which typically include polypropylene and polyethylene. ASTM D7508/7508M is the standard specification for synthetic fibers, including synthetic macrofibers and microfibers. ASTM D7508/7508M requires the minimum tensile strength of synthetic macrofibers to be 50,000 psi (345 MPa), whereas there are no restrictions on the tensile strength of microfibers. Synthetic macrofibers have typical diameters in the range of 0.012 to 0.04 in. (0.3 to 1.0 mm) and a length in the range of 1/2 to 2.5 in. (12 to 65 mm). The specified dosage for synthetic macrofibers depends on the application and the required engineering performance, as described in later chapters. These fibers are available in various configurations such as rope or tape filaments and they may be twisted or embossed. Bond to the concrete is achieved primarily through friction; however, chemical bonding in concrete has been reported.

Synthetic microfibers are mainly used for controlling cracks from plastic shrinkage (and sometimes drying shrinkage). Their contribution to the mechanical properties of hardened concrete is insignificant. These fibers are relatively fine with a typical diameter in the range of 0.0004 to 0.012 in. (0.01 to 0.3 mm) and a length in the range of 1/8 to 2 in. (3 to 50 mm). Synthetic microfibers are used in relatively small dosages, typically between 0.5 and 1.5 lb/yd^3 (0.3 and 0.9 kg/m^3) or 0.03 to 0.1 percent by volume. Some manufacturers carry blended fibers that typically includes synthetic microfibers (for plastic shrinkage crack control) and macrofiber (steel or synthetic) for enhancing the mechanical properties of concrete.

3.2—Performance of FRC

Unlike reinforcing bars, fibers are uniformly distributed in concrete and the average distance between fibers is much smaller than the typical spacing for reinforcing bars. As a result, tensile stresses are borne by the fibers at very early stages of the cracking process and, therefore, crack development and patterns can change with respect to plain or conventionally reinforced concrete. The decision on the type, material, size, geometry, and dosage for fibers depends on the application as well as the environmental exposure. Ultimately, the performance of FRC should be evaluated using standard test methods for the application for which it is used.

Fiber reinforcement can change the post-crack response of concrete from brittle to ductile under various types of loads, including compression, tension, flexure, and impact (Bonakdar et al. 2013). The addition of fibers to concrete can specially improve the crack resistance and toughness under tensile and flexural loads. Therefore, they can be used for structural purposes and to reduce the amount of required conventional reinforcement. The reduction of steel reinforcing bars is more significant in structures with a multiple degree of redundancy (di Prisco et al. 2009). In flexure, no major change takes place up to the cracking point of concrete. Fibers cannot be expected to modify the behavior of uncracked elements because fiber reinforcement mechanisms are mainly activated through crack development. When uncracked, FRC can be assumed to be homogeneous and isotropic, but this assumption does not hold for FRC in its cracked state. After cracking, fibers bridge the cracks and start to carry tensile stresses, giving load-bearing capacity to FRC in its cracked state. This is usually referred to as residual strength or post-cracking strength. Steel and synthetic macrofibers have been shown to significantly improve the post-crack response of concrete, providing residual strength values that can be used for design purposes (Buratti et al. 2011). With the same mixture design, fiber type, and concrete strength, higher fiber contents provide higher values of residual strength in tension or flexure, as long as the mixture can properly accommodate the fibers. The type and geometry of fibers also affect the post-crack properties of FRC. Ultra-high-performance FRC (UHPFRC) incorporates high-strength concrete and high dosages of fibers that can result in strain-hardening, as explained in later chapters. For steel fibers, dosages of more than approximately 60 lb/yd^3 (36 kg/m^3) and for synthetic macrofibers, dosages of more than approximately 15 lb/yd^3 (9 kg/m^3) may provide strain-hardening properties. Self-consolidating concrete, using plasticizers, is typically used for accommodating high dosages of fibers, resulting in improved mechanical and durability properties (Naaman and Reinhardt 1996).

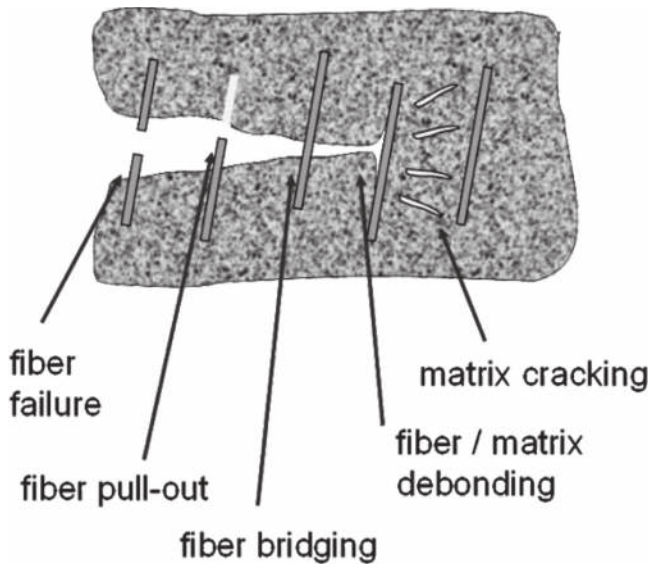

Fig. 3.2a—Schematics of the mechanism in which fiber reinforcement works.

The stages involved in FRC failure are schematically shown in Fig. 3.2a and are summarized in the following: 1) crack forms in cement matrix; 2) debonding and sliding between fiber and matrix; 3) bonded fiber bridging the crack; 4) frictional sliding, deformation of anchorage, and eventual fiber pullout; and 5) potential fiber rupture under tension. The term "failure" can be associated with the final stage when fibers are no longer able to resist the stresses, or when their strength is ignored in design. For specific types or geometries of fibers, only some of the described stages may occur. The load or stress level carried by fibers in a cracked concrete section is referred to as residual load or residual stress. The area under the load-deflection curves is the energy absorbed by the FRC and is referred to as toughness, which is used for design purposes. Figure 3.2b shows different stages of crack control for an FRC beam under a flexural load test. The beam was purposely cracked to much larger crack widths, than required, to demonstrate the ability of fibers in bridging the crack under sustained loads.

Contrary to reinforcing bars or welded mesh, most fibers are designed to deform and slip without failing in tension. Fibers are activated as soon as cracks are formed in the concrete. The main advantage of adding fibers to concrete is

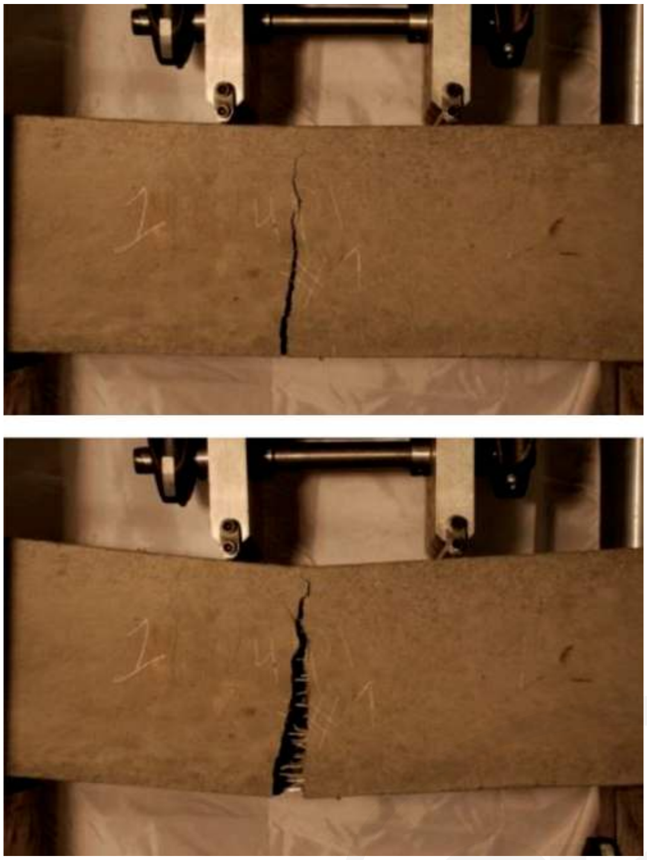

Fig. 3.2b—Crack control (bridging) in FRC beam under flexural loading. Note that in a standard test, the crack width is limited to approximately 0.12 in. (3 mm), whereas this beam was additionally loaded to show crack control at wide crack widths up to 1 in. (25 mm).

that they generate a post-cracking tensile/flexural strength in concrete, and this is true under both static and impact loads (Schrader 1981; Gopalaratnam and Shah 1986; Dey et al. 2014). As such, FRC is characterized by substantial ductility and toughness (Shah and Rangan 1970). The flexural toughness and post-crack residual strength of FRC depend on several factors, including fiber material, dosage, aspect ratio, geometry, bond characteristics, and concrete properties. The choice of fiber type may be affected by the long-term performance of FRC for certain applications. This includes the effect of sustained loads (creep) as well as environmental exposure resulting in corrosion. Steel fibers typically do not exhibit creep behavior under normal service conditions at temperatures below approximately 700°F (370°C). Synthetic fibers, however, are considered viscoelastic materials and are more susceptible to creep than steel fibers. If a relatively high stress level is maintained for considerable time, polymeric materials may behave viscously and will creep. For FRC elements with lower stress levels or structures with continuous support (such as slabs-on-ground or shotcrete), creep may not be a determining factor and synthetic macro-fibers may be used. For applications such as elevated slabs-on-pile without continuous support, only steel fibers have been used. The combined use of conventional steel reinforcement and fibers can considerably reduce the long-term deformations under sustained loads and the crack widths with a positive effect on the durability of concrete.

3.3—Standard test methods for FRC

If crack control under plastic shrinkage is the intended function of the fibers, ASTM C1579 can be used. The effectiveness of fibers in controlling the drying shrinkage (under restraint) and reducing the crack widths can be determined following ASTM C1581/C1581M. In these two tests, the effectiveness of fibers in reducing the crack width is determined and expressed in a percentage versus control (plain concrete). If higher levels of crack control and post-crack flexural capacity are expected from fibers, FRC beams or panels should be tested using ASTM C1609/C1609M and ASTM C1550. Equivalent European test methods are BS EN 14651:2005 and BS EN 14488:2006, respectively.

Performing a direct tension test (static or fracture) is ideal and desirable for FRC; however, a proper tension test is extremely difficult for cement-based materials because of the potential slippage or crushing of concrete at the grips, or heterogeneous nature of FRC. As an accepted alternative, flexural tests are conducted and the results are used for back-calculating the tensile properties. These flexural tests are designed to obtain the complete pre- and post-crack response of FRC. All the existing design tools for FRC use the test parameters obtained from some type of a bending test. This document describes two test methods that are widely used for measuring the residual strength, the parameter that is implemented in FRC design: ASTM C1609/C1609M and BS EN 14651:2005.

3.3.1 *ASTM C1609/C1609M: Standard Test Method for Flexural Performance of Fiber-Reinforced Concrete (Using Beam with Third-Point Loading)*—This test measures the complete pre- and post-crack flexural response of FRC beams using accurate deflection to control the test (closed-loop control). The test is typically performed on 6 x 6 x 20 in. (150 x 150 x 500 mm) FRC beams with a span of 18 in. (450 mm). Two points of loading (four-point bending) are used until reaching a midpoint deflection of 1/150th of the span (L)—that is, 0.12 in. (3 mm). Figure 3.3.1 shows the schematics of a typical ASTM C1609/C1609M test and a beam subjected to flexure (bending). The following parameters are determined from the test and used in characterizing FRC, which includes the peak strength as well as the residual strength values at L/600 (0.03 in. [0.75 mm]) and L/150 (0.12 in. [3 mm]). Note that b is the width and h is the height of the beam. At least three replicate beams should be tested for determining these parameters, though testing six beams is recommended for achieving a representative average value for residual strength of FRC.

a) P_P: peak flexural load (maximum load), lbf (kN)

b) P^D_{600}: FRC flexural residual load at a deflection of L/600, lbf (kN)

c) P^D_{150}: FRC flexural residual load at a deflection of L/150, lbf (kN)

d) f_P: peak flexural strength, psi (MPa)

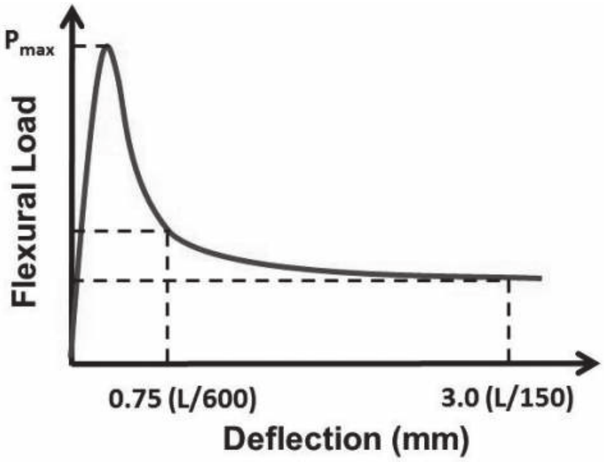

(a)

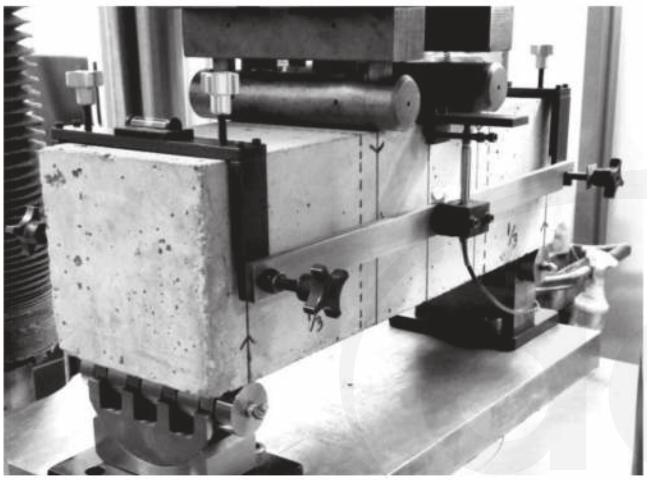

(b)

Fig. 3.3.1—(a) Schematics of a typical ASTM C1609/C1609M test result (strain-softening FRC); and (b) FRC beam under four-point flexural test. (Note: 1 in. = 25 mm.)

e) f^D_{600}: FRC flexural residual strength at a deflection of L/600, psi (MPa)

f) f^D_{150}: FRC flexural residual strength at a deflection of L/150, psi (MPa)

g) T^D_{150}: FRC flexural toughness up to a deflection of L/150, lb-in. (joule)

h) $R^D_{T,150}$: FRC equivalent flexural strength ratio at a deflection of L/150 (%), calculated as shown in Eq. (3.3.1a) from the toughness value (hence, subscript T). The term $R_{e,3}$ has also been used in the literature to represent this parameter, referring to 0.12 in. (3 mm) deflection.

$$R^D_{T,150} = \frac{150 \times T^D_{150}}{f_P \cdot b \cdot h^2} \quad (3.3.1a)$$

i) $f_{e,3}$: FRC equivalent flexural strength at a deflection of L/150, psi (MPa), calculated as shown in Eq. (3.3.1b). This term is not directly defined in ASTM C1609/C1609M; however, it has been widely used in the literature, referring to 0.12 in. (3 mm) deflection.

$$f_{e,3} = f_P \times R^D_{T,150} \quad (3.3.1b)$$

The residual strength measured from this test is in flexure and proper conversion factors should be used to determine the residual strength in tension. This is further discussed in Chapter 4.

3.3.2 *BS EN 14651:2005: Test and Design Methods for Steel Fiber-Reinforced Concrete*—This test method was originally introduced by RILEM TC 162-TDF (2003), and the test parameters are widely used for design in several design codes and specifications, especially when the design is based on a limited crack width. The test is performed on 6 x 6 x 22 in. (150 x 150 x 550 mm) FRC beams with a span of 20 in. (500 mm) and a small notch of 1 in. (25 mm) depth at the midspan. The notch is used as a crack initiator and the deflection and crack-mouth opening displacement (CMOD) are measured at the midspan during the test. The beam is tested under closed-loop control with one point of loading (three-point bending) until reaching a CMOD of 0.14 in. (3.5 mm). The parameter $F_{R,i}$ is the residual load at point i on the load-CMOD curve, and $f_{R,i}$ is the equivalent flexural residual strength. For example, $f_{R,3}$ is the residual strength at point i = 3, where the crack opening or CMOD is 0.1 in. (2.5 mm). In Eq. (3.3.2), L is the loading length (span), b is the width, and h_{sp} is the net height of the beam (total height – notch height). Figure 3.3.2 shows the schematics of a typical test for BS EN 14651:2005 and a beam under flexural (bending) test. A subscript i of 1, 2, 3, or 4 points out to crack opening or CMOD values of 0.02, 0.06, 0.1, or 0.14 in. (0.5, 1.5, 2.5, or 3.5 mm) that are used for specific crack width, desired in the design of a concrete member. At least three replicate beams should be tested for determining these parameters, though testing six beams is recommended for achieving a representative average value for residual strength of FRC.

a) F_{max}: peak flexural load (maximum load), lbf (kN)

b) $F_{R,i}$: FRC flexural residual load at point i, lbf (kN)

c) $f_{R,i}$: FRC flexural residual strength at point i, calculated as shown in Eq. (3.3.2), psi (MPa)

$$f_{R,i} = \frac{3F_{R,i} \cdot L}{2b \cdot h_{sp}^2} \quad (3.3.2)$$

It should be noted that a modified version of this test has been conducted without a notch, where higher dosages of fibers were used, resulting in multiple cracks (strain-hardening).

3.4—Strain softening and strain hardening

Low to moderate dosages of fibers provide enough resistance for bridging one main crack in a tension or flexural test and the response is referred to as strain softening. During strain softening, the residual strength gradually declines as the beam deflection and crack width increase. Strain softening FRC has a post-cracking tensile stress that is lower than its ultimate tensile strength. With special fiber reinforcement that incorporates higher dosages, anchoring mechanisms, and improved bond strengths, the fibers can

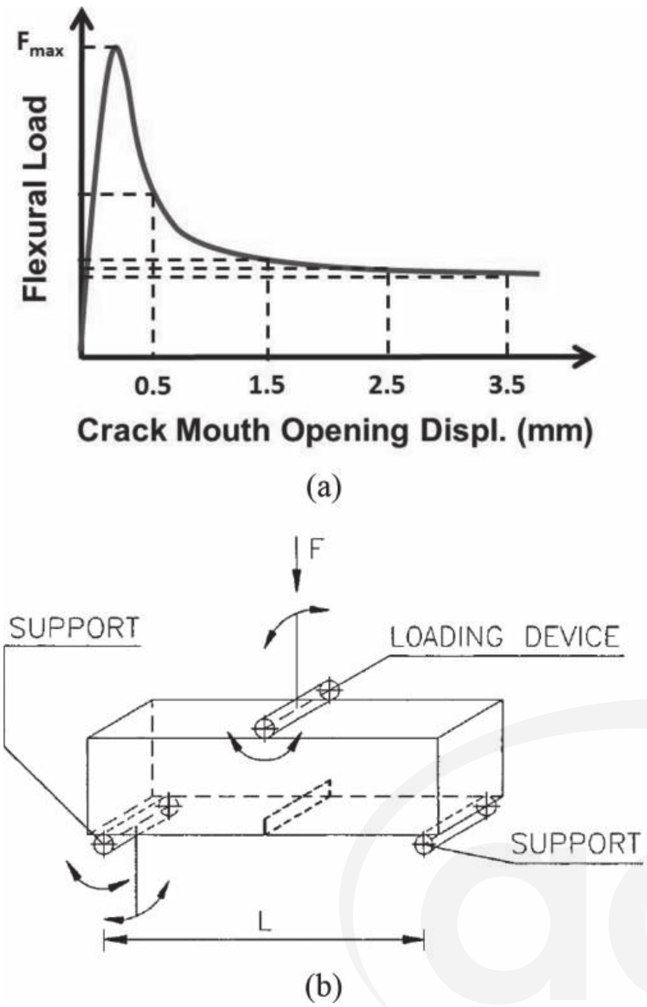

Fig. 3.3.2—(a) Schematics of typical BS EN 14651:2005 test results (strain-softening FRC); and (b) schematics of FRC beam under three-point flexural test. (Note: 1 in. = 25 mm.)

provide extra resistance for bridging several cracks and redistributing the stresses. This response is known as strain hardening. During strain hardening, the residual strength gradually increases as the deformations and crack widths get larger up to a point of failure. With the advancements of new generations of fibers and chemical admixtures, it is possible to produce strain-hardening FRC with post-cracking tensile stress that is higher than the cracking stress of concrete.

Two simplified stress-crack opening constitutive laws may be deduced from a uniaxial tensile test—plastic rigid behavior or linear post-cracking behavior (hardening or softening), as shown schematically in Fig. 3.4a. In these graphs, σ is the tensile stress, w is the crack width, and w_u is the ultimate crack width for a given design. With the assumption of rigid-plastic response, fibers are providing a constant residual strength after cracking, regardless of the crack width. In this model, f_{Ftu} represents the ultimate tensile residual strength. With the assumption of linear response, the residual strength provided by the fibers after cracking can either decrease (strain softening) or increase (strain hardening) as the crack grows. In this model, f_{Fts} represents the

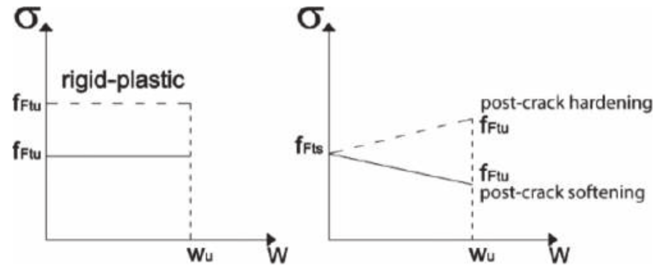

*Fig. 3.4a—Simplified post-crack stress-crack width relationship for FRC, obtained from uniaxial test, showing softening and hardening behaviors (*fib *2013).*

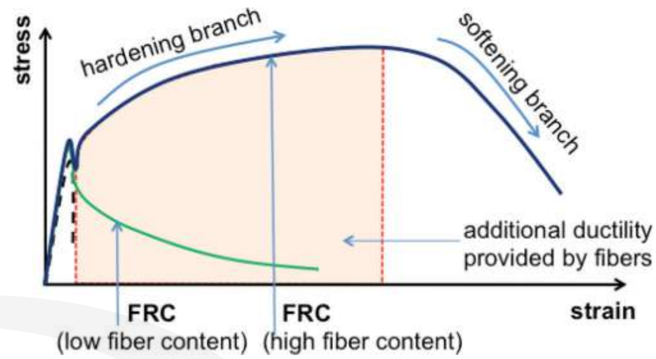

Fig. 3.4b—Fiber contribution to tensile/flexural performance, obtained from flexural test, showing softening and hardening behaviors.

serviceability residual strength, defined as the post-cracking strength for certain crack widths.

Figure 3.4b shows the flexural stress-strain curves for two different fiber dosages. The dotted line, which corresponds to the unreinforced concrete, shows a brittle failure once the cracking load is reached. The green line corresponds to FRC with relatively low fiber dosage; there is no such brittle failure, but once the first crack occurs, load-carrying capacity is gradually decreased (softening behavior). The blue line represents the behavior of FRC with relatively high fiber dosage; after the cracking load is reached, concrete will sustain the loads, and fibers make it possible to carry increasing loads (hardening branch) until a maximum stress value (ultimate load) is reached in the post-peak region, which is higher than the cracking load of concrete. After that, load-carrying capacity gradually decreases (final softening branch). Because of the contribution of fibers, the material is capable of absorbing a great deal of additional deformation energy (shadowed region under the curve) compared to its unreinforced counterpart.

The frontier between softening behavior and hardening behavior depends on several factors, including fiber material, geometry, and dosage. In relation to that, di Prisco et al. (2009) have pointed out that, for the same fiber type, the residual strength depends significantly on the number of fibers crossing active cracks and on their orientation. Fibers are therefore to be selected based on the type of member and the load conditions. Curves in Fig. 3.4c illustrate FRC flexural response, but similar comments can be made in relation to its tensile behavior. However, the fact that a certain FRC

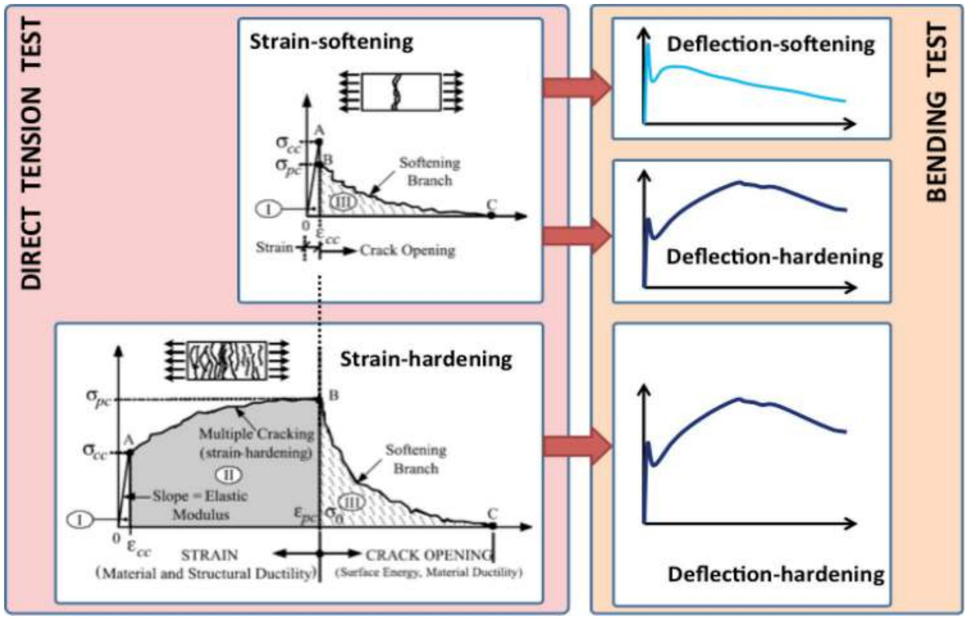

Fig. 3.4c—Different possibilities of FRC response in tension and flexure (Naaman 2007).

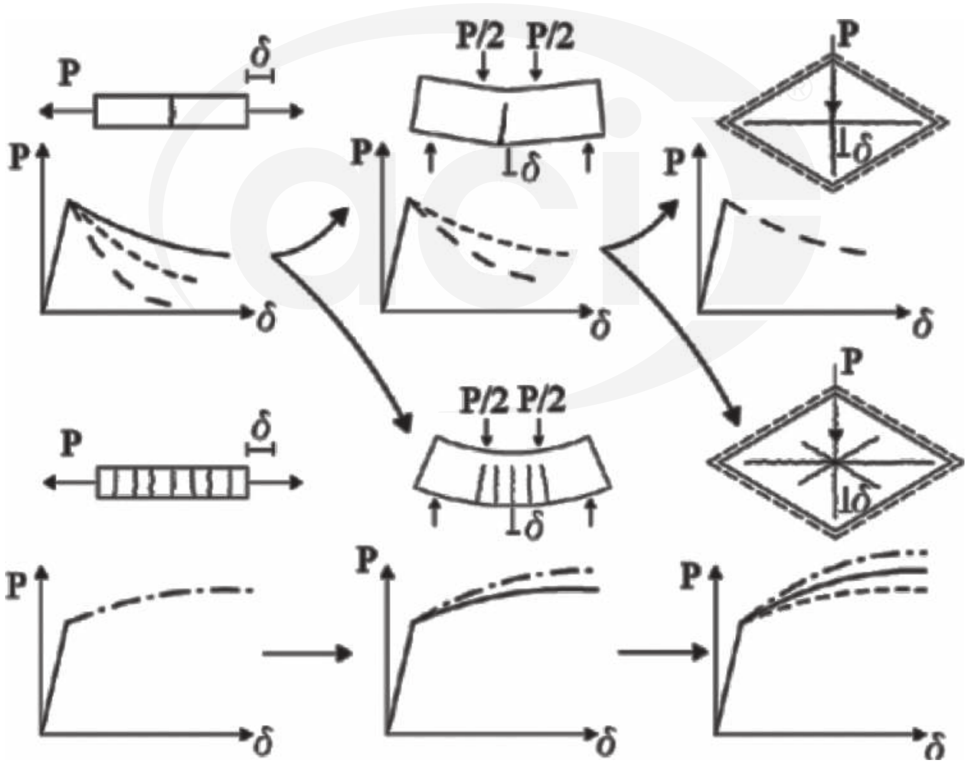

Fig. 3.4d—Schematics of strain softening and strain hardening in FRC under tension, flexure, and a system (Model Code 2010 [fib 2013]). The top three show strain-softening behavior; the bottom three show strain-hardening response.

presents a hardening flexural behavior does not necessarily imply tensile behavior to be hardening as well.

Under certain conditions, a bending-hardening response of a structure can be achieved even with a tension-softening or bending-softening material. This means that only structures with sufficient redistribution capabilities can be designed with softening materials in accordance with Model Code 2010 (*fib* 2013). If system ductility cannot be proven for structures reinforced with fibers alone, Model Code 2010 (*fib* 2013) requires conventional reinforcement to achieve a ductile response of the structure. These are schematically shown in Fig. 3.4d for FRC under tension, flexure, and a system. The top three graphs show strain-softening behavior while the bottom three graphs show strain-hardening response for the three cases.

CHAPTER 4—DESIGN CONCEPTS AND GUIDES

4.1—Design concepts

The design of FRC and the introduction of its properties in structural calculations are based on the performance of the composite material and not individual fibers. Construction feasibility and short-term and long-term performance requirements may limit the types and dosage of fibers in certain applications. Attention should be paid to the residual strength as the main parameter, as it is affected by the type and dosage of fibers as well as the properties of concrete. By using a performance-based calculation and specification, the engineer can ensure proper performance from FRC as a composite material. Similar to conventional reinforcement with bars in a cracked concrete section, fibers bridge the cracks and restrain their growth, providing post-crack load-carrying capacity under tension, bending, and shear.

Material properties such as residual strength are determined from standard beam tests described in the previous chapter. These properties are then inserted into the equations, as presented in this chapter, for determining the performance of the FRC and the corresponding load-carrying capacity. Test programs should be conducted in such a way that an appropriate design strength can be established, which includes proper allowance for the uncertainties covered by the partial safety factors in conventional design. Generally, it will be necessary to establish the influence of material strengths on the behavior and their variability so that a characteristic (and thus design) response can be derived. When testing is carried out on elements significantly smaller or larger than the prototype, size effects should be considered in the interpretation of results. Attention should be paid to material behavior at both limit states: ultimate limit state (ULS) for strength requirements as well as serviceability limit state (SLS) for crack width and deflection limits.

Tensile strength of plain concrete is insignificant and therefore is not taken into account in the design of a conventional reinforced concrete section. Adding steel or synthetic macrofibers to concrete provides post-cracking tensile strength; hence, the effective tensile strength of FRC is used in the design process. As explained previously, performing a proper tension test is difficult and flexural tests are conducted alternatively. Residual tensile strength is then derived from the measured residual flexural strength by means of conversion factors. The following provides a summary of the design concepts and procedures; however, more details on the tensile stress-strain response of FRC and its correlation with the flexural test data can be found in ACI 544.8R.

4.2—Tensile stress-strain response for FRC

Many studies have been conducted to determine the stress-strain curve of FRC in direct tension (Shah et al. 1978; Gopalaratnam and Shah 1987b); however, there is no standard test method recognized by ASTM. The idealized tensile stress-strain diagram used in this document is the same as one proposed by RILEM TC 162-TDF (2003) shown in Fig. 4.2. The values that define this constitutive model are based on average or characteristic values that are, in turn, used in the design process. The key points of the compression side of the diagram are obtained directly from the standard compressive cylinder test. For the tension side of the diagram, the key points are indirectly obtained from a flexural test.

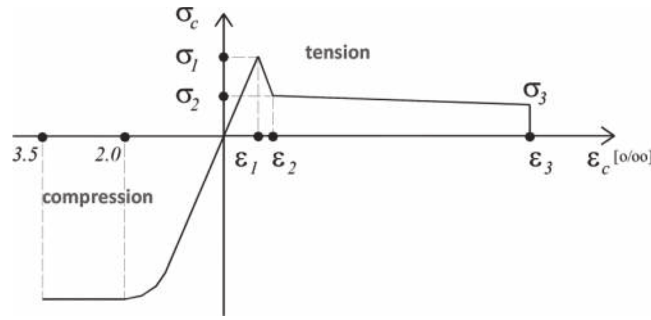

Fig. 4.2—Schematics of a typical stress-strain diagram for FRC in uniaxial tension and compression, according to RILEM TC 162-TDF (2003) and Vandewalle (2003).

a) σ_1 and ε_1—tensile stress and corresponding strain at onset of first cracking

b) σ_2 and ε_2—stress and strain at the onset of the stable softening branch

c) σ_3 and ε_3—stress and strain at the end of the softening branch

4.3—Correlation of tensile and flexural response for FRC

Experimental studies have been performed on FRC specimens using both direct tension and bending tests, showing the correlation between the tensile and flexural response in the post-crack region of material behavior (Vandewalle 2003). These studies have shown that the flexural residual strength of FRC in a cracked section is typically between 2.5 and 3 times its tensile residual strength. This is because of the stress gradient in a stress block analysis (Naaman 2007). For design purposes, the tensile residual strength should be calculated from the flexural residual strength obtained from a beam test. Such calculations should follow the provisions of the design approach being applied for FRC and in practice; the conversion factor is typically taken between 0.4 and 0.33. The comparison of numerical studies with experiments confirms such relationships (Mobasher et al. 2014).

Typically, two design levels can be considered for FRC: 1) serviceability limit state (SLS) at smaller deflections, corresponding to smaller crack widths in the range of 0.016 to 0.04 in. (0.4 to 1.0 mm); and 2) ultimate limit state (ULS) at larger deflections, related to larger crack widths in the range of 0.08 to 0.14 in. (2.0 to 3.5 mm). Higher values of residual strength become necessary for SLS, as the crack widths should be maintained smaller. Hence, the specified residual strength for FRC is determined based on the desired limit state.

The two test methods described in Chapter 3 are commonly used for determining the flexural residual strength of FRC after concrete has cracked. The parameters obtained from these two tests can be used for design, as explained in this chapter. When ASTM C1609/C1609M is used to char-

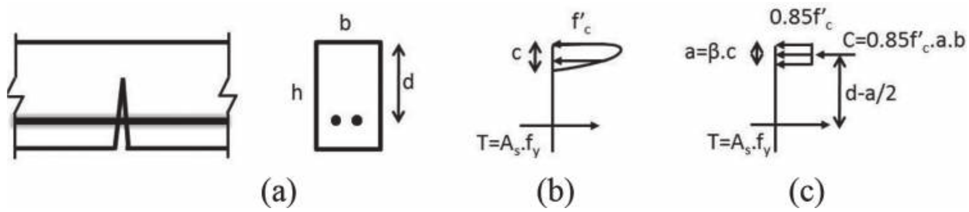

Fig. 4.4—Schematics of stress block for a cracked reinforced concrete flexural member without fibers: (a) reinforced concrete beam section; (b) actual distribution of normal stresses; and (c) simplified distribution of normal stresses.

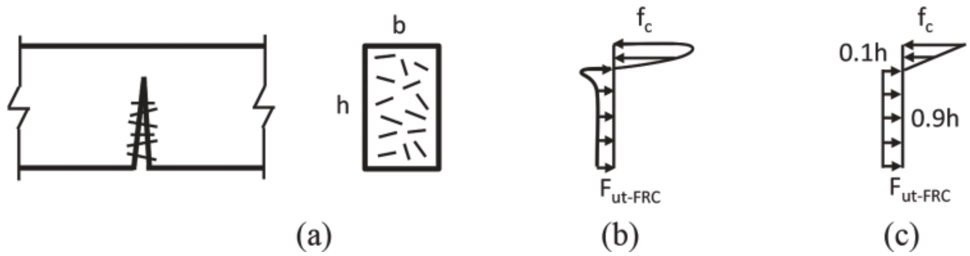

Fig. 4.5—Schematics of stress block for a cracked FRC flexural member. (a) FRC beam section; (b) actual distribution of normal stresses; and (c) simplified distribution of normal stresses.

acterize FRC, parameters such as f_{600}^{D}, f_{150}^{D}, and $R_{D,150}^{T}$ (or $f_{e,3}$) are used for design and specification. This test and the corresponding design method are typically used in North America. In Europe and some other countries, the BS EN 14651:2005 test method is more common and the design parameters are $f_{R,1}$, $f_{R,2}$, $f_{R,3}$, and $f_{R,4}$. The implementation of these parameters in the design process is explained in the following sections.

4.4—Design of RC for flexure (stress block)

The nominal bending moment for a conventional reinforced concrete section without fibers, $M_{n\text{-}RC}$, is calculated according to Eq. (4.4) from the force equilibrium in the cross section as shown in Fig. 4.4. As illustrated schematically, Fig. 4.4(a) is a RC beam section without fibers, Fig, 4.4(b) shows the actual distribution of normal stresses, and Fig. 4.4(c) shows the simplified distribution of normal stresses in the cracked section. After concrete has cracked, the compressive force C is carried by concrete (above the neutral axis) and the tensile force T is carried by reinforcing bar (below the neutral axis). It should be noted that the stress block is only accurate for the calculation of the ultimate moment, not for deriving a moment-curvature relation. The tensile capacity of plain concrete is negligible and is not taken into account in these calculations.

$$M_{n\text{-}RC} = A_s \cdot f_y \cdot \left(d - \frac{a}{2}\right) \tag{4.4}$$

where $a = \dfrac{A_s \cdot f_y}{0.85 f_c' \cdot b}$

Note that once the flexural strength of concrete is reached, it will crack and all the tensile forces are provided by the steel reinforcement. When designed based on load and resistance factors (LRFD), the design moment capacity of the reinforced concrete section, $\phi M_{n\text{-}RC}$, should be greater than the factored moment M_u applied to the section: $\phi M_{n\text{-}RC} > M_u$. The reduction factor ϕ depends on the type of the member and its failure mode, should be determined based on ACI 318 or other building codes, and is typically between 0.65 and 0.9 for flexural members.

4.5—Design of FRC for flexure (ASTM C1609/C1609M, in conjunction with RILEM TC 162-TDF [2003])

The same stress block concept can be applied to an FRC section. ASTM C1609/C1609M is performed to obtain the required design parameters. The nominal bending moment for an FRC section, $M_{n\text{-}FRC}$, is calculated according to Eq. (4.5a) and (4.5b) from the force equilibrium in the cross section, as shown in Fig. 4.5. As presented schematically, Fig. 4.5(a) is an FRC beam section reinforced with fibers, Fig. 4.5(b) shows the actual distribution of normal stresses, and Fig. 4.5(c) shows the simplified distribution of normal stresses in the cracked section. The compressive stresses are carried by concrete and the tensile stresses are carried by reinforcing fibers. The distribution of the compressive stresses for FRC is simplified as triangular rather than rectangular because of the composite action of fibers and concrete above the neutral axis. The tensile strength of FRC is much higher than that of plain concrete and therefore is taken into account in these calculations. For ULS, the ultimate tensile strength of cracked FRC, $f_{ut\text{-}FRC}$, can be taken as 0.37 times its flexural residual strength, f_{150}^{D} (or f_{e3}), measured from ASTM C1609/C1609M test as shown in Eq. (4.5a). The moment capacity of a cracked FRC section is shown in Eq. (4.5b), developed in conjunction with the similar method used by RILEM

TC 162-TDF (2003) and Vandewalle (2003). If FRC is designed for smaller crack widths under SLS requirements, other parameters such as f^D_{600} can be used that correspond to smaller deflection in the beam test. The choice of the design limit (ULS versus SLS) and the related design parameter depends on the application and serviceability requirements.

$$f_{ut\text{-}FRC} = 0.37 f^D_{150} \quad (4.5a)$$

$$M_{n\text{-}FRC} = f^D_{150} \times \frac{bh^2}{6} \quad (4.5b)$$

Sometimes the equivalent residual strength $f_{e,3}$ is used instead of the residual strength f^D_{150}. The former parameter ($f_{e,3}$) is an indication of the total energy absorption (flexural toughness) in a beam test and is usually used for the design of FRC members that are continuously supported such as slabs-on-ground and shotcrete. The latter parameter (f^D_{150}) is the actual value of flexural residual strength at a given deflection or crack width. This parameter is commonly used for FRC members without continuous support, including beams, suspended slabs, and precast segments. The value of f^D_{150} can be slightly smaller than $f_{e,3}$, which results in a more conservative design. The choice between the two parameters depends on the application, design criteria, and safety requirements. The design moment capacity of FRC, $\phi M_{n\text{-}FRC}$, should be greater than the factored moment M_u applied to the section: $\phi M_{n\text{-}FRC} > M_u$. Note that compared with conventionally-reinforced concrete, these ϕ factors may require adjustments prior to use for FRC members for compression-controlled and tension-controlled failure modes. More conservative (lower values) of ϕ factors should be used for FRC members without continuous support such as beams, suspended slabs, and precast. For FRC members with continuous support, such as slabs-on-ground and shotcrete, higher values of ϕ factors may be used.

Example: Assume a 6 in. (150 mm) slab-on-ground exposed to tensile shrinkage and temperature stresses. Consider various reinforcement ratios of 0.05, 0.1, and 0.15 percent and find the required flexural residual strength $f_{e,3}$ for FRC to provide the same level of crack control as Grade 60 steel.

Tensile force provided by steel: $F_{ts} = \frac{A_s}{b \cdot h} \cdot F_y = \rho \cdot F_y = 60{,}000\rho$

The required values of tensile and flexural residual strengths have been calculated for the given steel reinforcement ratios shown in Table 4.5. Note that in this example, the flexural residual strength is 0.37 times the required post-crack tensile strength as described earlier in this section.

Example: Assume an 8 in. (200 mm) precast panel reinforced with No. 4 bars at 16 in. (bar diameter 12.7 mm, spaced at 400 mm) placed in midsection to provide post-crack moment capacity. Find the value of f^D_{150} for FRC to provide the same level of post-crack flexural strength as reinforcing bar. Assume 5000 psi (35 MPa) concrete and

Table 4.5—Typical calculation of FRC residual strength values for crack control

Steel reinforcement ratio ρ	Requires tensile residual strength		FRC flexural residual strength	
%	psi	MPa	psi	MPa
0.05	30	0.2	81	0.6
0.10	60	0.4	162	1.1
0.15	90	0.6	243	1.7

Grade 60 (414 MPa) steel and a moment capacity factor of 0.9 for steel.

Factored moment capacity provided by steel:

$$\phi M_{n\text{-}RC} = \phi A_s F_y \left(d - \frac{a}{2}\right)$$
$$= 0.9 \times 0.147 \times 60{,}000 \times \left(\frac{8}{2} - \frac{0.17}{2}\right) = 31{,}120 \text{ lb-in.}$$

where $a = \frac{A_s F_y}{0.85 f_c' b} = \frac{0.147 \times 60{,}000}{0.85 \times 5000 \times 12} = 0.17 \text{ in.}$

Ultimate moment capacity for FRC:

$$\phi M_{n\text{-}FRC} = \phi M_{n\text{-}RC} = 31{,}120 \text{ lb-in.} = \phi f^D_{150} \frac{bh^2}{6}$$
$$\rightarrow f^D_{150} = \frac{6 M_{n-FRC}}{\phi bh^2} = \frac{6 \times 31{,}120}{0.9 \times 12 \times 8^2}$$
$$= 270 \text{ psi (1.86 MPa)}$$

4.6—Design of FRC for flexure (Model Code 2010 [*fib* 2013])

The FRC design may be performed using the moment-crack width relationship obtained from BS EN 14651:2005 test on notched beams using Model Code 2010 (*fib* 2013) design guidelines summarized herein. The nominal moment for an FRC section, $M_{n\text{-}FRC}$, is calculated according Eq. (4.6a) through (4.6d) from the force equilibrium in the cross section, as shown in Fig. 4.6. As presented schematically, Fig. 4.6(a) is an FRC beam section reinforced with fibers; Fig. 4.6(b) shows the distribution of flexural stresses, whereas Fig. 4.5(c) shows the simplified distribution of normal stresses in the cracked section. A constant value of tensile residual strength f_{Ftu} is used for ultimate state design. Two models are proposed for calculating the post-crack tensile strength of FRC in this method. In the first model, called simplified rigid-plastic, the ultimate tensile strength of FRC, $f_{Ftu\text{-}FRC}$, is taken as a constant value of one-third times the flexural residual strength of FRC, $f_{R,3}$, that is measured from the BS EN 14651:2005 beam test. The formulas for calculating the tensile strength and nominal bending moment are shown in Eq. (4.6a) and (4.6b), respectively. The second model assumes a linear relationship between the residual strength and the crack width both for serviceability and ultimate limit

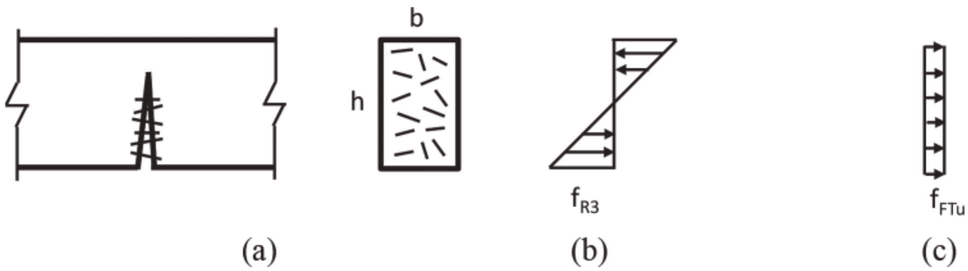

Fig. 4.6—Schematics of stress block for a cracked FRC flexural member: (a) FRC beam section; (b) distribution of flexural stresses; and (c) simplified distribution of normal stresses.

design of an FRC section. The formulas for calculating the tensile strength and nominal bending moment are shown in Eq. (4.6c) and (4.6d), respectively. Attention should be paid to the state of design: serviceability limit state (SLS) versus ultimate limit state (ULS) in choosing the correct equations. It is noted that design according to Model Code 2010 (*fib* 2013) only covers fiber materials with a Young's modulus not significantly affected by time or temperature, or both. In addition, minimum requirements apply such as $f_{R,1}/f_L > 0.4$ and $f_{R,3}/f_{R,1} > 0.5$, in which f_L is the limit of proportionality (LOP) calculated according to Eq. (3.3.2). The rules given by Model Code 2010 (*fib* 2013) are based on experience with steel fiber-reinforced concrete only.

Using rigid-plastic model (for ULS only):

$$f_{Ftu\text{-}FRC} = \frac{f_{R,3}}{3} \tag{4.6a}$$

$$M_{nu\text{-}FRC} = f_{R,3} \cdot \frac{bh_{sp}^2}{6} \tag{4.6b}$$

Using linear model (for SLS and ULS):

$$\begin{cases} f_{Fts-FRC} = 0.45 f_{R,1} \\ f_{Ftu-FRC} = (0.45 f_{R,1}) - \dfrac{w_u}{CMOD_3} \geq 0 \\ (0.45 f_{R,1} - 0.5 f_{R,3} + 0.2 f_{R,1}) \end{cases} \tag{4.6c}$$

$$\begin{cases} M_{ns\text{-}FRC} = f_{R,1} \cdot \dfrac{bh_{sp}^2}{6} \\ M_{nu\text{-}FRC} = f_{R,3} \cdot \dfrac{bh_{sp}^2}{6} \end{cases} \tag{4.6d}$$

Example: BS EN 14651:2005 test has been conducted on FRC beams and the values of $f_{R,1}$ = 1000 psi (6.9 MPa) and $f_{R,3}$ = 800 psi (5.5 MPa) have been reported. What are the nominal moment capacities of this FRC for SLS and ULS conditions? Assume a maximum crack width w_u = 0.06 in. (1.5 mm) and use the linear model approach.

Residual tensile strength of FRC under SLS and ULS:

$$\begin{cases} f_{Fts\text{-}FRC} = 0.45 f_{R,1} = 0.45 \times 100 \\ \quad = 450 \text{ psi (3.1 MPa)} \\ f_{Ftu\text{-}FRC} = (0.45 f_{R,1}) - \dfrac{w_u}{CMOD_3} \\ \quad \cdot (0.45 f_{R,1} - 0.5 f_{R,3} + 0.2 f_{R,1}) \\ \quad = 450 - \dfrac{0.05}{0.1}(450 - 0.5 \times 800 + 0.2 \times 1000) \\ \quad = 325 \text{ psi (2.2 MPa)} \end{cases}$$

Nominal moment capacity of FRC under SLS and ULS:

$$\begin{cases} M_{ns\text{-}FRC} = 1000 \times \dfrac{6 \times 5^2}{6} = 25{,}000 \text{ lb-in. (9000 N-m)} \\ M_{nu\text{-}FRC} = 20{,}000 \text{ lb-in. (7200 N-m)} \end{cases}$$

4.7—Design of FRC for flexure-hybrid reinforcement

Hybrid reinforcement (using bars plus fibers) could be a viable option for the design and construction of concrete members with high levels of reinforcement and steel congestion. A portion of reinforcing bars may be substituted with fibers to allow for better consolidation of concrete and a faster construction. A recent structural application of hybrid reinforcement was published by Kopczynski and Whiteley (2016), where steel fibers were used to replace diagonal bars in shear wall coupling beams in a high-rise building. Full-scale tests and computer simulations showed an improved strength and ductility in the concrete members with hybrid reinforcement, whereas the total amount of reinforcing bars was reduced by 40 percent. The moment capacity of a hybrid FRC section is calculated taking into account the contribution of both steel bars and fibers, as shown in a general form in Fig. 4.7. As presented schematically, Fig. 4.7(a) is beam section reinforced with bars and fibers, and Fig. 4.7(b) shows the distribution of normal stresses in a cracked section. The compressive stresses are carried by concrete while the tensile stresses/forces are carried by the hybrid action of bars and fibers. Such calculations can be done for serviceability limit state (SLS) and ultimate limit state (ULS) following the general guidelines described in 4.5 and 4.6. The general form of nominal moment capacity

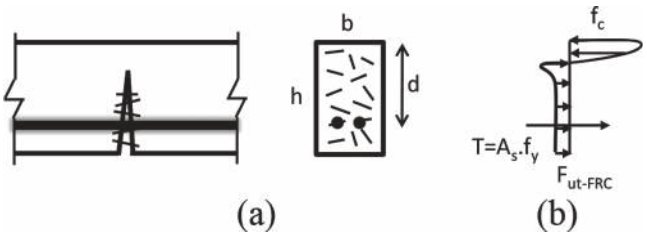

Fig. 4.7—Schematics of stress block for a cracked flexural member with hybrid reinforcement: (a) beam section; and (b) distribution of normal stresses and forces from fibers and reinforcing bar.

of a member with hybrid reinforcement (M_{n-HFRC}) is shown in Eq. (4.7). Various configurations for hybrid reinforcement are possible; more information can be found in Model Code 2010 (*fib* 2013), Vandewalle (2000c), Tiberti et al. (2008), Barros et al. (2015), and Mobasher et al. (2015b).

$$M_{n-HFRC} = M_{n-RC} + M_{n-FRC} \tag{4.7}$$

4.8—Design of FRC for shear

The design aspects of FRC for shear in flexural members where longitudinal bars are used in conjunction with fibers as shear reinforcement are presented herein. The use of fibers as shear reinforcement in reinforced concrete beams has been the focus of several studies, as mentioned in 1.3.7. Referring to the results of a full-scale study done by Parra-Montesinos (2006), ACI 318 recognizes the use of steel fibers as shear reinforcement in place of stirrups in flexural members with $f_c' < 6000$ psi (40 MPa) and maximum beam height of 24 in. (600 mm). According to ACI 318 Section R26.12.5, steel fibers should have an aspect ratio between 50 and 100 and provide a minimum $R^D_{T,150}$ of 75 percent when tested according to ASTM C1609/C1609M. The lower limit for the shear capacity provided by SFRC is $3.5\sqrt{f_c'}b_wd$ psi ($0.29\sqrt{f_c'}b_wd$ MPa), where b_w is the width and d is the effective height of the beam. Shoaib et al. (2014) showed that concrete beams with higher f_c' and greater overall height than ACI 318 limits and those that did not satisfy the $R^D_{T,150}$ criteria were able to provide a shear capacity of at least $2.0\sqrt{f_c'}b_wd$ psi ($0.17\sqrt{f_c'}b_wd$ MPa).

Model Code 2010 (*fib* 2013) Section 7.7.3.2 has summarized the shear design considerations for SFRC. For concrete members with conventional longitudinal reinforcement but without shear reinforcement, Eq. (4.8) may be used for calculating the shear capacity. According to this code, it is possible to eliminate minimum amount of conventional shear reinforcement (stirrups) if the ultimate tensile residual strength of FRC is sufficiently high—that is, $f_{ut-FRC} > (0.6)f_c^{(1/2)}$ psi ($f_c^{(1/2)}/20$ MPa).

$$V_{FRC} = 26.8\times\left\{\frac{0.18}{\gamma_c}k_s\left[100\rho\left(1+7.5\frac{f_{ut-FRC}}{f_t}\right)f_c\right]^{\frac{1}{3}}+0.15\sigma_{cp}\right\}\cdot b\cdot d$$

(in.-lb units)

$$V_{FRC} = \left\{\frac{0.18}{\gamma_c}k_s\left[100\rho\left(1+7.5\frac{f_{ut-FRC}}{f_t}\right)f_c\right]^{\frac{1}{3}}+0.15\sigma_{cp}\right\}\cdot b\cdot d$$

(SI units)

(4.8)

where $V_{FRC} > (v_{min} + 0.15\sigma_{cp})bd$, where $v_{min} = 0.035k_s^{(3/2)}f_c^{(1.2)}$.

In this equation, γ_c is concrete partial safety factor without fibers; k_s is size effect factor and is equal to $1 + (8/d)^{(1/2)} \leq 2.0$ (in.-lb units) ($1 + (200/d)^{(1/2)} \leq 2.0$ [SI units]); ρ is longitudinal reinforcement ratio and is equal to $A_s/(b \cdot d)$; f_{tu-FRC} is the ultimate tensile residual strength of FRC; f_t and f_c are tensile and compressive strength values of plain concrete, respectively, and σ_{cp} is average normal stress acting on concrete cross section due to loading or prestressing. Note that ACI 318 has a more conservative approach and higher safety factors than Model Code 2010 (*fib* 2013) for these shear calculations.

Example: Assume a concrete beam with $b = 12$ in. (300 mm), $d = 20$ in. (500 mm) with three No. 4 (bar diameter: 12.7 mm) bars in the tension zone. Concrete strength $f_c = 4000$ psi (27.5 MPa) and $f_t = 400$ psi (2.75 MPa). Determine the shear capacity of this section: 1) without fibers; 2) fibers with $f^D_{150} = 200$ psi (1.38 MPa); and 3) fibers with $f^D_{150} = 400$ psi (2.75 MPa). Assume $\gamma_c = 1$ and zero normal stress on the beam.

$$k_s = 1+\sqrt{\frac{8}{d}} = 1+\sqrt{\frac{8}{20}} = 1.63 < 2$$

$$\rho = \frac{A_s}{A_c} = \frac{3\times\pi\times(0.5^2)/4}{12\times 20} = 0.00246,\ \text{or } 0.02\%$$

1) $F_{ut-FRC} = 0$ psi (0 MPa) with no fibers;

$$V_{FRC} = 26.8\times$$
$$\left\{\frac{0.18}{1.0}\times1.63\times\left[100\times0.00246\times\left(1+7.5\times\frac{0}{400}\right)\times4000\right]^{\frac{1}{3}}+0\right\}$$
$$\times 12\times 20 = 18,770 \text{ lbf (83.5 kN)}$$

2) $F_{ut-FRC} = 0.37 \times 200 = 74$ psi (0.51 MPa) with f^D_{150} of 200 psi (1.38 MPa)

$$V_{FRC} = 26.8\times \left\{\frac{0.18}{1.0}\times 1.63\times\left[100\times 0.00246\times\left(1+7.5\times\frac{74}{400}\right)\times 4000\right]^{\frac{1}{3}}+0\right\}\times 12\times 20 = 25,090 \text{ lbf (111.6 kN)}$$

3) $F_{ut\text{-}FRC} = 0.37 \times 400 = 148$ psi (1.02 MPa) with f_{150}^D of 400 psi (2.75 MPa)

$$V_{FRC} = 26.8\times \left\{\frac{0.18}{1.0}\times 1.63\times\left[100\times 0.00246\times\left(1+7.5\times\frac{148}{400}\right)\times 4000\right]^{\frac{1}{3}}+0\right\}\times 12\times 20 = 29,230 \text{ lbf (130.0 kN)}$$

The FRC with f_{150}^D of 200 psi (1.38 MPa) increases the shear capacity of this section by 33 percent and the FRC with f_{150}^D of 400 psi (2.75 MPa) can increase the shear capacity up to 55 percent compared to a section with no fiber reinforcement. Note that the value of 200 psi (1.38 MPa) for f_{150}^D may be too low to satisfy the requirement of ACI 318 for using fibers as the sole means of shear reinforcement, yet it can still provide an increase in shear strength.

Altoubat et al. (2009) have shown that synthetic macrofibers can also provide the required shear capacity in flexural members when used at the proper dosage. More recently, Altoubat et al. (2016) investigated the use of synthetic macrofibers as the shear reinforcement in flexural members, showing that some of the existing empirical formulas (developed for steel fibers) overestimate the shear strength of FRC with synthetic fibers; however, the equations in Model Code 2010 (*fib* 2013) could be safely used for such a prediction. Other shear capacity models have been proposed that may be suitable when the mechanical properties of FRC are available. Shoaib et al. (2012) developed a shear capacity model for members with hooked-end steel fibers that can account for the observed size effect in shear. Dinh et al. (2010) and others have also validated various shear capacity models. For FRC members with both flexural and shear reinforcement, the contribution of fibers can be added (that is, $V_{HFRC} = V_s + V_{FRC}$).

4.9—Parametric-based design for FRC

Soranakom and Mobasher (2009) as well as Mobasher (2011) presented a simplified parametric model based on serviceability limit state (SLS) and ultimate limit state (ULS) criteria for the design of FRC flexural members. This model can be implemented both for strain-softening and strain-hardening FRC. As an extension to the model, one can also consider a combination of fibers and plain reinforcement in the context of hybrid reinforcement concrete (HRC), which addresses structural members that combine continuous reinforcement with randomly distributed chopped fibers in the matrix. An analytical model for predicting flexural behavior of HRC, which is applicable to conventional reinforced concrete and FRC, is presented by Mobasher et al. (2015b).

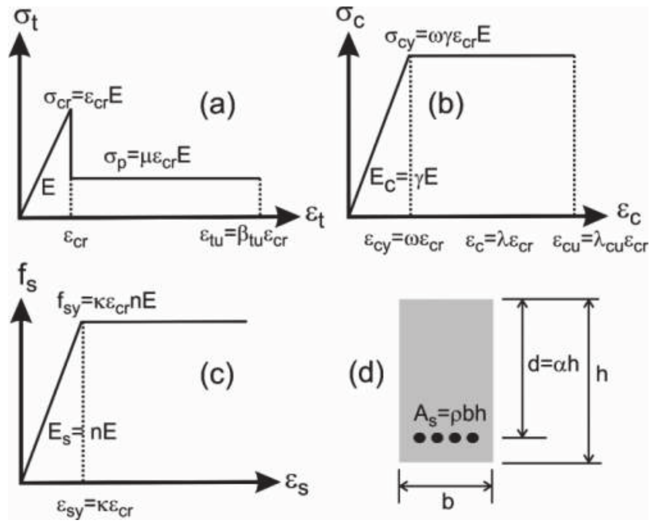

Fig. 4.9a—Material model for singly reinforced concrete design: (a) tension model; (b) compression model; (c) steel model; and (d) beam cross section.

Parameter-based tensile and compressive strain-stress diagrams of composite and steel sections are shown in Fig. 4.9a for a typical plain or hybrid-FRC cross section. Figure 4.9a represents the material (a) tensile and (b) compressive constitutive stress strain responses for FRC as well as the reinforcement. The tensile response of matrix in Fig. 4.9a(a) is represented as elastic with a stiffness of E up to first-crack strain and strength of ε_{cr} and σ_{cr}, respectively. This point is followed by a constant magnitude of residual stress contributed by the pullout slip response of fibers across the crack and is defined by parameter μ (represented as a fraction of tensile strength), resulting in the stress measure of $\mu\sigma_{cr}$. The compressive response in Fig. 4.9a(b) is represented as an elastic-plastic response with an initial modulus defined as γE up to compressive strength of $\omega\mu\sigma_{cr}$, where parameter ω represents the ratio of compressive to tensile strain, and in most of the cases, elastic modulus for tension and compression are equal; therefore, $\gamma = 1$. Thus, parameter ω can be considered the ratio of compressive to tensile strength; $\sigma_{cy} = \omega\sigma_{cr}$, as well. Figure 4.9a(c) represents the elastic perfectly plastic model for steel reinforcement bars. The arrangement of the reinforcing bars within a cross section of width b and depth h shown in Fig. 4.9a(d) shows that the depth of center of gravity of the reinforcement is at a distance $d = \alpha h$.

Figure 4.9b shows the different stages of elastic and inelastic zones of tension and compression response based on a linear strain distribution. The constitutive response relates the strains to curvature, stresses, forces, and, thus, the bending moment. After solving for the depth of neutral axis, the value of moment and curvature are calculated at each range of applied strain and used to construct the moment-curvature response for a given section. The parameters for the constitutive models are obtained from either ASTM C1609/C1609M or BS EN 14651:2005, based on the recom-

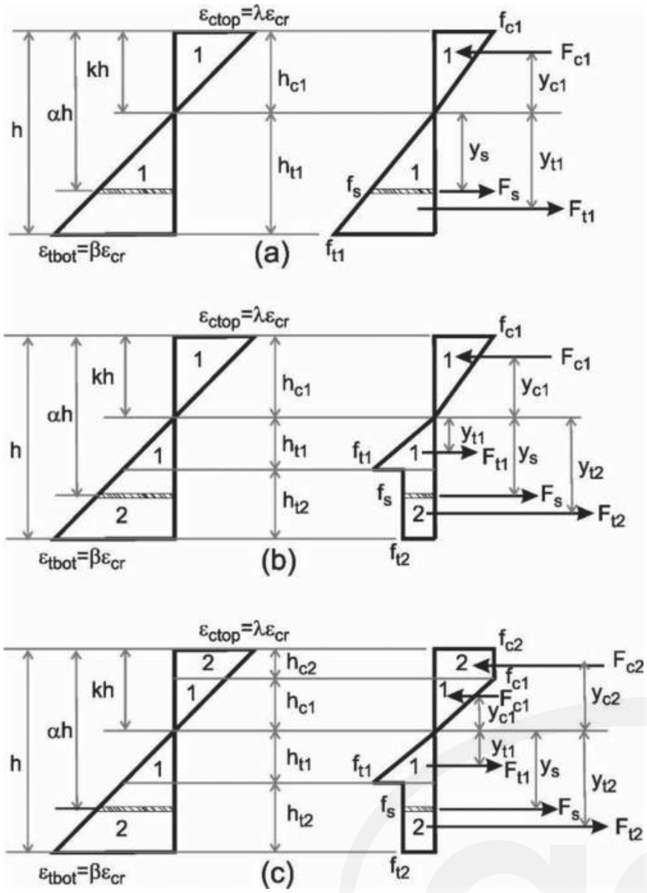

Fig. 4.9b—Stress and strain diagrams at three ranges of normalized top compressive strain λ: (a) elastic for compression and tension ($0 < \lambda < 1$); (b) elastic for compression but nonlinear for tension ($1 < \lambda < \omega$); and (c) plastic for compression and nonlinear for tension ($\lambda > \omega$).

mendations of a parametric design method as discussed in ACI 544.8R.

A minimum of three parameters are needed for this model and include the ratio of compressive to tensile strength ω, the post-crack tensile residual strength $\mu\sigma_{cr}$, and the allowable compressive or tensile strain from a serviceability point of view ($\beta_{tu}\varepsilon_{cr}$ or $\lambda_{cu}\varepsilon_{cr}$). Using these parameters, the location of neutral axis, moment capacity, and curvature of the section can be obtained at any imposed strain.

The solution for the plain fiber-reinforced concrete section is presented first for the case in Fig. 4.9b(c), specified by a cracked section under tension and the maximum compressive strain at the elastic-plastic compression zone ($\varepsilon_c > \lambda\varepsilon_{cr}$, $\lambda > \lambda_{cr} = \omega$). For the given applied strain distribution, the location of neutral axis is assumed as kd, and using the strain and stress profile across the section, the force equilibrium equation is obtained. The neutral axis depth k is found by solving the equilibrium of net internal forces, or $F_s + F_{c1} + F_{c2} + F_{t1} + F_{t2} = 0$ representing the forces due to internal stresses as defined in Fig. 4.9b. For a specified serviceability limit for maximum allowable compressive strain $\varepsilon_c = \lambda_{cu}\varepsilon_{cr}$, the neutral axis depth is obtained as

$$k = \frac{2\mu\lambda_{cu}}{-\omega^2 + 2\lambda_{cu}(\omega+\mu) + 2\mu - 1} \quad (4.9a)$$

Equation (4.9a) is for the plain FRC section, and the full derivation for a hybrid reinforced case is presented by Mobasher et al. (2015b). The magnitude of the moment, M_n, is obtained by taking the first moment of internal forces about the neutral axis, $M_n = F_{c1}y_{c1} + F_{c2}y_{c2} + F_{t1}y_{t1} + F_{t2}y_{t2}$, calculated as shown in Eq. (4.9b) and (4.9c) as

$$M_n = \left((3\omega\lambda_{cu}^2 - \omega^3 + 3\mu\lambda_{cu}^2 - 3\mu + 2)\frac{k^2}{\lambda_{cu}^2} - 3\mu(2k-1) \right)\cdot M_{cr} \quad (4.9b)$$

$$M_{cr} = \frac{\sigma_{cr}bh^2}{6} \quad (4.9c)$$

If an asymptotic analysis is conducted to compute the moment capacity in the limit case, a simplified design equation for normalized moment capacity is obtained. This resembles a case when the cracked section in flexure opens significantly to go beyond serviceability limit; however, due to the presence of fibers, the section can still transmit the flexural load applied. The moment capacity in this case is defined by the limit case of compressive cracking strain λ_{cu} reaching a relatively large number (Soranakom and Mobasher 2009). To simplify the calculation of several specified moments, the neutral axis parameter k_∞ can be computed by substituting $\lambda_{cu} = \infty$ to obtain the normalized ultimate limit moment m_∞, as shown in Eq. (4.9d). The equation for ultimate moment capacity is derived by substituting m_∞ for m_{cu}. Thus, the deign equation for nominal moment capacity M_n is expressed in Eq. (4.9d).

$$\begin{aligned} k_\infty &= \lim_{\lambda\to\infty} k = \frac{\mu}{\omega+\mu} \\ m_\infty &= \frac{3\omega\mu}{\omega+\mu} \\ M_n &= m_\infty M_{cr} = \frac{3\omega\mu}{\omega+\mu}M_{cr} \end{aligned} \quad (4.9d)$$

The LRFD basis for the ultimate strength design is based on the reduced nominal moment capacity $\phi_p M_n$ exceeding the factored demand moment M_u, which is determined by linear elastic analysis using factored load coefficients according to ACI 318-14 Section 9.2. A strength reduction factor ϕ_p is applied to the post-crack tensile strength, and a tentative value of $\phi_p = 0.75$ to 0.9 has been used based on statistical analysis of limited test data in the earlier work. To further simplify Eq. (4.9d) from the previous equations, an empirical relationship between tensile and compressive strength may also be used—that is, $f_t' = 6.7\sqrt{f_c'}$ (in.-lb units) ($0.62\sqrt{f_c'}$ in SI units). Therefore, the normalized compressive strength ω is shown as:

$$\omega = \frac{\gamma E\omega\varepsilon_{cr}}{E\varepsilon_{cr}} \approx \begin{cases} \dfrac{f_c'}{f_t'} = \dfrac{0.85f_c'}{6.7\sqrt{f_c'}} = 0.127\sqrt{f_c'} & (f_c' \text{ in psi}) \\ \dfrac{f_c'}{f_t'} = \dfrac{0.85f_c'}{0.56\sqrt{f_c'}} = 1.518\sqrt{f_c'} & (f_c' \text{ in MPa}) \end{cases} \quad (4.9e)$$

By substituting for ω, the expression for nominal moment capacity as a function of the post crack tensile strength μ and ultimate compressive strength f_c' of Eq. (4.9d) is obtained for a given ultimate moment as shown in Eq. (4.9f).

$$M_n = \left[\frac{6\mu\sqrt{f_c'}}{\xi\mu + 2\sqrt{f_c'}}\right]M_{cr} \quad (4.9f)$$

where ξ = 15.8 in in.-lb units and 1.32 in SI units.

For a typical fiber-based system, the apparent residual strength of FRC in flexure is assumed to be approximately three times its residual strength in tension—that is, $f_{eq,3} = 3\mu\sigma_{cr}$ (Mobasher et al. 2014; ACI 544.8R). M_n can be obtained according to Eq. (4.9g).

$$M_n = \left[\frac{6f_{eq,3}\sqrt{f_c'}}{\xi(f_{eq,3} + 2.54f_c')}\right]M_{cr} \quad (4.9g)$$

where ξ = 15.8 in in.-lb units and 1.32 in SI units.

Alternatively, a general power relationship between tensile and compressive strength is represented as:

$$f_t' = n(f_c')^k$$

$$M_n = \left[\frac{3f_{eq,3}(f_c')^{1-k}}{(n)(f_{eq,3} + 3f_c')}\right]M_{cr} \quad (4.9h)$$

For example, if the concrete mixture is designed with $f_{eq,3}$ = 250 psi (1.72 MPa) and a concrete strength of 5000 psi (35 MPa), values of n = 6 and k = 0.5 are used for correlation of tensile and compressive strengths, and $M_n = 0.35M_{cr}$ as the limit state of the moment capacity. Note that the value computed is a multiplier of the first crack moment according to Eq. (4.9g) is computed. Eq. (4.9f) can also be rearranged as

$$\mu = \frac{2m_\infty\sqrt{f_c'}}{6\sqrt{f_c'} - m_\infty\xi} \quad (4.9i)$$

where $m_\infty = M_n/M_{cr}$.

Equations to determine the moment-curvature relationship, ultimate moment capacity, and minimum flexural reinforcement ratio were explicitly derived (Mobasher et al. 2015b). Figure 4.9b presents all three distinct material models used in the derivation of analytical expressions of moment-curvature and load-deflection of HRC beams, which includes

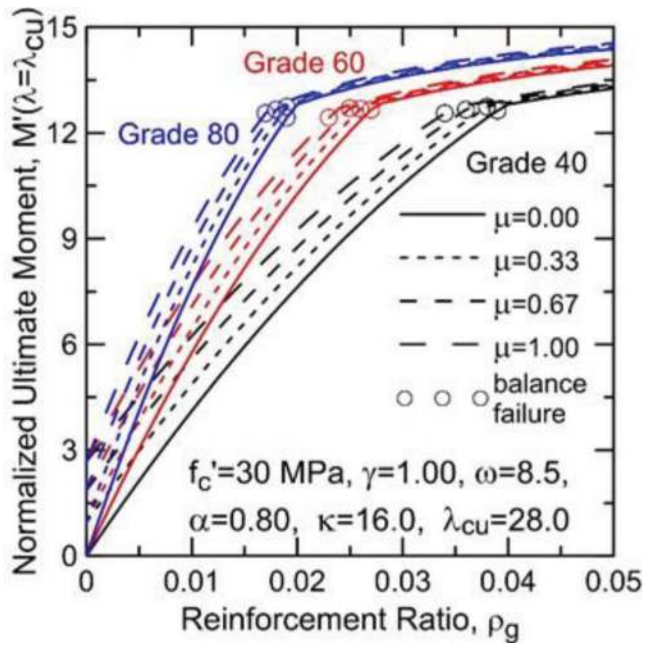

Fig. 4.9c—Design chart for normalized ultimate moment capacity (determined at $\lambda = \lambda_{cu}$) for different levels of post-crack tensile strength μ and reinforcement ratio.

the interaction of compression and tension failure of FRC as well as failure by tension yielding of steel. The ultimate moment capacity as a function of residual tensile strength and reinforcement can be used as a convenient design tool for combinations of reinforcement, calculated as shown in Eq. (4.9j). Using this equation, an analytical expression for minimum reinforcement ratio $\rho_{g,min}$ for conventional reinforced concrete is also obtained. For example, using parameters μ = 0, γ = 3/4, and ω = 6, Eq. (4.9k) is obtained with represents the minimum reinforcement as a function of depth location and its stiffness (steel or FRP).

$$M_n \approx m_\infty M_{cr} = \frac{6\rho_g n\kappa(\mu\alpha - \mu + \alpha\omega) + 3\omega\mu - 3(\rho_g n\kappa)^2}{\omega + \mu}M_{cr} \quad (4.9j)$$

$$\rho_{min} = \frac{9\alpha - \sqrt{81\alpha^2 - 6}}{2\alpha n\kappa} \quad (4.9k)$$

Figure 4.9c shows a design chart for the parametric design model with various grades of steel. Flexural design using this chart requires ultimate moment M_u due to factored loads normalized with respect to cross-sectional geometry. For any combination of normalized residual tensile strength μ, grade of steel, and reinforcement ratio ρ_g, the allowable demand ultimate moment capacity M_u' is obtained from this chart. Results are then scaled to numerical values using the section cracking moment M_{cr}. An excel spreadsheet has been developed by Mobasher et. al (2015a) as a design guide for both the FRC and HRC. Several examples are presented in the following section.

CHAPTER 5—DESIGN FOR SPECIFIC APPLICATIONS

5.1—Slabs-on-ground

Slabs-on-ground are one of the main applications of fibers as the sole method of reinforcement in concrete. Various types of slabs-on-ground such as residential and commercial floors as well as roads and pavements may experience cracking before ultimate loads are applied. Such causes include drying shrinkage, thermal variations, environmental exposures (for example, freezing and thawing and alkali-silica reaction), stress concentration at reentrant corners, and repetitive loading (fatigue). The three-dimensional reinforcement that is provided by steel or synthetic macrofibers improves the crack resistance of concrete, specifically near the surface, resulting in a longer service life.

ACI 360R discusses the details and calculations for fiber reinforcement and only a summary is presented herein. The thickness of the slab is traditionally designed based on the empirical equations provided by Westergaard (1923, 1925, 1926), taking into account the subgrade modulus, the concrete flexural strength, and the applied loads. Despite the conservatisms of this method, concrete slabs often end up with cracks that are formed as a result of shrinkage or thermal stresses or other nonstructural causes. Therefore, reinforcement in the form of steel bars, wire mesh, or macrofibers is used to provide crack-width control and post-crack load-carrying capacity to the concrete slab (ACI 360R-10 Chapter 8). Minimum dosages of fibers are intended to control the cracks from shrinkage and thermal stresses. For steel fibers, the minimum dosage is typically 17 to 20 lb/yd^3 (10 to 12 kg/m^3) and for synthetic macrofibers, this value is approximately 3 to 4 lb/yd^3 (1.8 to 2.4 kg/m^3). Higher dosages of fibers will additionally provide bending moment capacity and flexural toughness to the section after cracking.

Steel fibers are typically used at a dosage between 17 and 60 lb/yd^3 (10 and 36 kg/m^3), whereas synthetic macrofibers are used in the range of 3 and 7.5 lb/yd^3 (1.8 and 4.5 kg/m^3) as the sole reinforcement for slabs-on-ground. The actual dosage for the fibers can be determined based on the required bending moment from the applied loads and subgrade properties. The residual strength values such as $f_{e,3}$ or $f_{R,i}$ or, more frequently, the residual strength ratio $R^D_{T,150}$ (same as $R_{e,3}$), is used for design and specifying FRC slabs. As explained in 3.3, $R^D_{T,150}$ (or $R_{e,3}$) is the ratio of flexural residual strength of FRC to the cracking strength of concrete and is commonly used for slab design. $R^D_{T,150}$ (or $R_{e,3}$) is an indication of post-crack moment capacity of a concrete slab due to fiber reinforcement. The yield-line method, which is discussed in detail in ACI 360R, accounts for the redistribution of moments and formation of plastic hinges in the slab after concrete has cracked. These plastic hinge regions develop at points of maximum moment and cause a shift in the elastic moment diagram. This allows for the efficient use of FRC after cracking and an accurate determination of its ultimate capacity. The yield-line method has been implemented for the design of slabs-on-ground where reinforcement is taken into account in redistribution of stresses in a cracked section (Meyerhof 1962; Lösberg 1978). For slabs reinforced with FRC, a similar model based on yield-line method was developed by Ghalib (1980). Simplified equations are presented in ACI 360R for the calculation of the moment capacity of FRC slabs under ultimate limit state (ULS). Three separate cases are shown in Eq. (5.1a), (5.1b), and (5.1c) for different load cases.

$$P_0 = 6\left[1+\frac{2a}{L}\right]M_0 \text{ (for load } P_0 \text{ in center of panel)} \tag{5.1a}$$

$$P_0 = 6\left[1+\frac{3a}{L}\right]M_0 \text{ (for load } P_0 \text{ on edge of panel)} \tag{5.1b}$$

$$P_0 = 6\left[1+\frac{4a}{L}\right]M_0 \text{ (for load } P_0 \text{ at corner of panel)} \tag{5.1c}$$

where L is the relative radius of stiffness (unitless) defined in Eq. (5.1d) in which K is the subgrade reaction modulus (lb/in^3 [N/mm^3]); E is the concrete modulus of elasticity (lb/in.^{2} [N/mm^2]), ν is concrete Poisson's ratio (unitless); and M_0 is expressed as shown in Eq. (5.1e). Other parameters have been defined previously.

$$L = \sqrt[4]{\frac{Eh^3}{12(1-\nu^2)K}} \tag{5.1d}$$

$$M_0 = \left[1+\frac{R^D_{T,150}}{100}\right]\times f_P \times \frac{bh^2}{6} \tag{5.1e}$$

The term in the bracket is considered an enhancement factor that accounts for the contribution of fibers in providing post-crack moment capacity in a slab-on-ground when the yield-line method is used. Some examples of slabs-on-ground reinforced with fibers only are shown in Fig. 5.1a through 5.1c.

Destrée et al. (2016) have presented a model to address shrinkage cracking and curling of slabs subjected to restraint by the ground level friction as well as the fiber bridging mechanism as two main factors. The main parameters affecting drying shrinkage can be divided into three categories: 1) concrete matrix properties such as the internal porosity, moisture content, potential free shrinkage strain, and tensile cracking strength; 2) internal cracking restraint due to the addition of fibers, modeled as a stress-crack width relationship; and 3) slab geometry and external boundary conditions in terms of evaporation rate and degree of restraint due to the base friction. The approach simulated the sequential formation of multiple cracks and opening responses due to imposed shrinkage strain. As shown in Fig. 5.1d, the primary parameters of the mechanics-based model were defined in terms of: 1) matrix cracking criterion; 2) frictional force at the base, modeled using a linear spring element that is modelled as a force-slip element; and 3) the

Fig. 5.1a—Concrete slab-on-ground reinforced with 4.3 lb/yd^3 (2.5 kg/m^3) of synthetic macrofiber (Cleveland Medical Mart and Convention Center, Cleveland, OH).

Fig. 5.1b—Concrete runway reinforced with 66 to 85 lb/yd^3 (39 to 50 kg/m^3) of steel fibers (O'Hare Airport runway, Chicago, IL).

Fig. 5.1c—Concrete canal reinforced with steel mesh (top) and 7.5 lb/yd^3 (4.5 kg/m^3) of synthetic macrofiber (bottom) (Pima-Maricopa Irrigation Project, Sacaton, AZ).

combination of fiber stiffness and interface bond-slip characteristics that is used as a stress-crack width relationship. Parametric studies on both models showed that the average crack width was reduced by increasing fiber content, interfacial bond strength, and frictional force by the base. The simulated results were compared with the field measurements of three slabs in service with different bay sizes of 118 x 118 ft, 131 x 131 ft, and 164 x164 ft (36 x 36 m, 40 x 40 m, and 50 x 50 m), respectively. Both methods accurately predicted the crack opening measured from field trials (Destrée et al. 2016).

FRC has also been used in topping slab applications such as bridge decks and parking garages. The thickness for topping slabs is typically small, making it impractical to maintain concrete cover for steel reinforcement. Fibers may be used as a sole reinforcement for topping slabs as a means of crack control, to provide the required post-crack moment capacity, or both. FRC overlays have been used for concrete or asphalt pavements. The design of FRC thin overlays bonded to asphalt pavements is discussed in Harrington and Fick (2014).

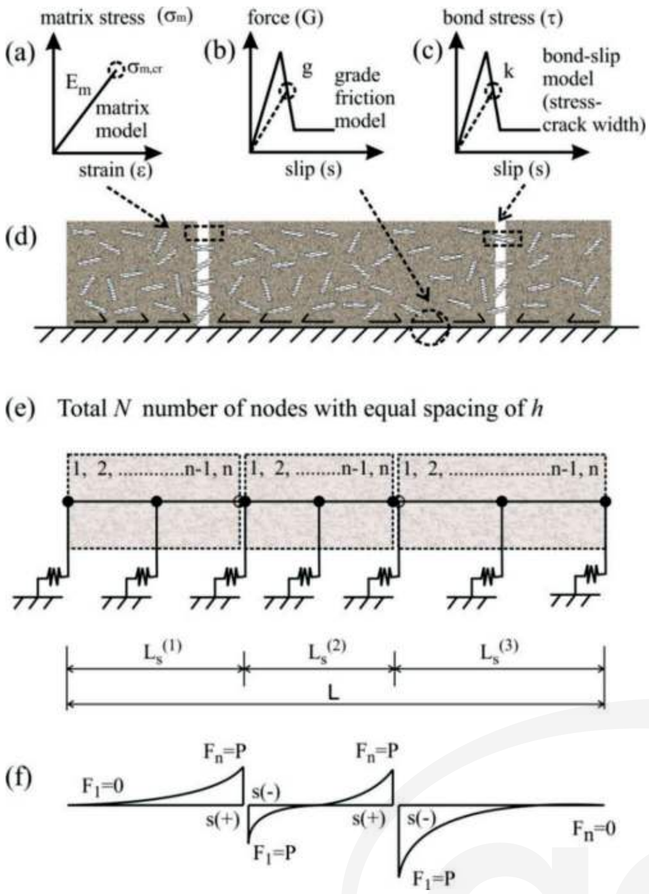

Fig. 5.1d—Parametric model for cracked FRC slab-on-ground: (a) matrix strength for cracking criterion; (b) nonlinear spring model simulating the frictional force; (c) bond-slip width model; (d) cracked concrete slab; (e) arrangement of nodes and springs; and (f) distribution of the slip in cracked specimens (Destrée et al. 2016).

5.2—Extended joint spacing

Fibers have been used successfully in the construction of concrete slabs-on-ground and topping slabs with fewer control joints (that is, extended joint spacing), compared to unreinforced concrete slabs. Extending the distance between control joints in concrete floors increases the potential for midpanel cracking. When fibers are used at sufficiently high dosages, however, the presence of numerous fibers in the concrete will bridge the cracks at the onset of formation and prevent the cracks from opening. Moreover, the high residual strength provided by fibers will ensure a desired post-crack moment capacity while keeping the crack widths smaller than a desired level. Successful use of high-aspect-ratio steel fibers in so-called jointless floors has been reported, as shown in Fig. 5.2a. Fibers may also be used in combination with steel bars or wire mesh for extending the joint spacing even further. Figure 5.2b shows a seamless FRC pavement using steel fibers and steel mesh in a port application.

Another approach for extending the joint spacing in floors is by the combined use of fibers and low-shrinkage concrete mixtures. Because drying shrinkage is one of the main reasons for cracking in concrete floors, reducing its value will allow for an increase in the spacing between control joints (Miltenberger and Attiogbe 2002). In this system, the required fiber dosage and the shrinkage of concrete are determined and specified for any given project. The factors affecting such values include the subgrade modulus, the expected loads, the slab thickness, and the desired joint spacing. The concrete mixture design can be optimized for reduced shrinkage by reducing the water content, reducing the cementitious materials, and using larger amounts of coarse aggregates (to reduce the required cement paste). Concrete additives such as shrinkage-reducing admixtures (SRAs) and shrinkage-compensating cements may be used for obtaining certain values of shrinkage. Concrete floors with no control joints (known as jointless floors) have been built using close-to-zero shrinkage and macrofibers (steel or synthetic). As stated in ACI 360R, when shrinkage-compensating concrete is used, slabs may be placed in areas as large as 10,000 ft^2 (930 m^2) with joint spacing of 100 ft (30 m) with minimized cracking. For more information on the use of shrinkage-compensating concrete, refer to ACI 223R. Extra attention should be paid to workmanship and construction practices such as adequate preparation of subgrade and proper placing and curing of concrete. Figure 5.2c shows a

Fig. 5.2a—FRC warehouse using high-aspect-ratio steel fibers at a dosage of 51 lb/yd^3 (30 kg/m^3) with extended joint spacing (Stykow, Poland).

Fig. 5.2b—Seamless 538,000 ft^2 (50,000 m^2) FRC pavement using high-aspect-ratio steel fibers at a dosage of 42 lb/yd^3 (25 kg/m^3) plus wire mesh (Port of Brisbane, Australia).

so-called jointless concrete slab warehouse using macrofibers and low-shrinkage concrete.

5.3—Elevated floors/slabs-on-piles

Design and construction methods of steel FRC (SFRC) slabs-on-piles have been fully discussed in ACI 544.6R. Applications of pile-supported slabs are quite common for areas where soil-structure interaction may create differential settlement, cracking, or long-term serviceability problems. The construction of slabs on closely-spaced piles is referred to as elevated ground slabs with span-depth ratios between 8 and 30, depending on the load intensity and the pile capacity. These slabs may be subjected to moderately high loading such as concentrated point loads, uniformly distributed loads, and dynamic loads such as forklift trucks (ACI 544.6R). Depending on the fiber performance, the occurring loads, and the support conditions, pile-supported floors can be reinforced with steel fibers alone or with a combination of steel fibers and bars. High dosages of steel fibers, typically between 85 and 170 lb/yd^3 (50 and 100 kg/m^3), have been used as the primary reinforcement for such elevated slabs. Steel fibers provide the required strength and ductility for the suspended slabs for the applied vertical and lateral loads. Steel bars are used in the slabs, between columns, for preventing collapse under special circumstances such as earthquake, impact, or explosion and are referred to as anti-progressive collapse bars. Construction of a multi-story elevated slab/floor using steel FRC is shown in Fig. 5.3, where steel fibers were used as the main reinforcement for the floors.

Fig. 5.2c—FRC warehouse with extended joint spacing using synthetic macrofibers at 7.5 lb/yd^3 (4.5 kg/m^3) and low-shrinkage concrete (Champaign, IL).

5.4—Composite steel decks

The steel reinforcement that is used for controlling shrinkage/temperature cracks in the concrete portion of a composite metal steel can be replaced by steel or synthetic macrofibers. The International Building Code (International Code Council 2015) refers to ANSI/SDI-C1.0:2014, which allows for using FRC in place of wire mesh for controlling cracks in concrete under shrinkage and thermal stresses. This document has prescriptive dosages for fibers with steel fibers at a minimum dosage of 25 lb/yd^3 (15 kg/m^3) and synthetic macrofibers at a minimum dosage of 4 lb/yd^3 (2.4 kg/m^3). However, lower dosages of steel fibers may be used upon testing and engineering approval. The steel deck only functions as tension reinforcement for positive moments and steel bars may be needed in areas of negative moment such as over the girders. Fibers, when used at an engineered dosage, can provide additional positive and negative moment as well as added shear capacity to a composite steel deck. If a continuous slab is desired, the negative reinforcement should be designed using conventional reinforced concrete criteria based on ACI 318 or other building codes. The fiber dosages mentioned in ANSI/SDI-C1.0:2014 may not replace the steel reinforcement that is welded to the shear studs to be a part of the shear diaphragm under seismic loads. However, full-scale tests have shown that higher dosages of steel and synthetic macrofibers can provide the same level of shear capacity as unwelded steel mesh in a composite steel deck

Fig. 5.3—Construction of a multi-story building with SFRC elevated slabs. Note that the only bars in the suspended slabs are between columns as anti-progressive collapse reinforcement and the slab itself is reinforced with steel fibers only (ACI 544.6R).

(Altoubat et al. 2016). Improved job safety and reduced risk of tripping for the construction workers is an important benefit of using FRC in place of steel mesh for composite steel decks. The construction of a typical composite deck using synthetic macrofibers is shown in Fig. 5.4.

5.5—Precast units

Using fibers in precast units is a popular choice by many producers for its technical and economic benefits. A variety of precast units can be made with FRC that include, but are not limited to, structural segments (deck panels and tunnel lining), water or waste management units (pipes, septic tanks, nuclear waste tanks, and flood retention), boxes (burial vaults, storm shelters, utility boxes, garages, and storage rooms), and decorative units (urban furniture, home furniture, sound wall panels, and shades). Structural capacity, fire resistance, and any other special performance requirements should be considered when choosing the right fiber type and FRC system. Precast units may have relatively thin sections and, therefore, placing steel reinforcing bar or mesh and consolidating concrete can be time-consuming and challenging. There could also be a potential for reducing the thickness as a result of the elimination of minimum concrete cover that is required for preventing corrosion of the steel reinforcement. The steel fibers that are exposed on the surface may corrode over time; however, the corrosion will be limited to only a few fibers and will not affect the structural integrity of the section. Fire protection requirements should be satisfied in the selection of thickness of FRC precast units.

Fig. 5.4—Concrete slab on metal deck reinforced with 4 lb/yd^3 (2.4 kN/m^3) synthetic macrofibers (22-story steel frame building, Newark, NJ).

Reinforcing with fibers allows for better automation of the production process, enhanced quality control, and improved characteristics of the final products. In some cases, while it may not be possible to completely replace the steel reinforcement, there may be the potential to reduce the amount of steel when hybrid systems (steel bars + fibers) are used. The National Precast Concrete Association (NPCA 2010, 2011, 2012) has some prescriptive language allowing the use of fiber reinforcement for precast wastewater units with steel fibers at dosages between 20 and 60 lb/yd^3 (12 and 36 kg/m^3) and synthetic macrofibers between 3 and 20 lb/yd^3 (1.8 to 12 kg/m^3). The actual dosages should be calculated according to the design requirements to provide the desired level of crack-width control, moment capacity of the section, or both. This has been discussed in detail in ACI 544.7R. Typical applications of FRC in precast concrete units are shown in Fig. 5.5a through 5.5c.

One of the uses of FRC is in precast segmental tunnel lining with extensive research and application experience, as discussed in detail in ACI 544.7R. Precast concrete segments are installed to support the tunnel bore behind the tunnel boring machine in soft ground and weak rock applications. FRC can be used to enhance the production and handling of precast concrete segments with minimizing human errors in placement of steel bars and improving worker safety. FRC can considerably improve the post-cracking behavior with better crack-control characteristics than conventional steel bar reinforced concrete (Minelli et al. 2011; Tiberti et al. 2014). Reinforcing bars are efficient for resisting localized stresses in the concrete segment; however, the distributed stresses are better dealt with by fiber reinforcement. Because both localized and distributed stresses are generally present in tunnel linings, hybrid reinforcement can offer an optimal solution (Plizzari and Tiberti 2006, 2007; de la Fuente et al. 2012). To date, the largest diameter of a segmental tunnel lining reinforced only with steel fibers is 40.7 ft (12.4 m). ACI 544.7R proposes a design procedure for FRC tunnel segments imposing the appropriate temporary and permanent load cases occurring during segment manufacturing, transportation, installation, and in-service load conditions due to earth pressure, groundwater, and surcharge loads. Full-scale tests including bending tests, as shown in Fig. 5.5d, and point load tests

Fig. 5.5a—Steel fibers used in tunnel lining segmental units.

Fig. 5.5b—Precast Pi section made with ultra-high-performance steel FRC (Jackway Park Bridge, IA).

Fig. 5.5c—Synthetic macrofibers used in precast wave breakers and septic tanks.

have been performed to verify the design and performance of segments for governing load cases.

5.6—Shotcrete

Soil and rock excavations can effectively be stabilized with FRC. It is also ideal for ground support in tunneling and mining due to its easy application. Shotcrete, in combination with other support elements, can provide early and effective ground support after blasting or excavating with early development of compressive and flexural strength and toughness. This can provide flexibility to allow for ground stabilization

Fig. 5.5d—Flexural testing of segmental units reinforced with steel fibers (Moccichino et al. 2006).

and the ability to conform to the natural irregular profile of the ground without formwork. The advantages of fiber-reinforced shotcrete over shotcrete reinforced with wire mesh or steel bars include labor and time savings, materials reduction, and improved safety. Steel and synthetic macrofibers are used in underground shotcrete with the primary objective of providing post-crack reinforcement and reduction in the number and width of shrinkage cracks that may eventually lead to water leakage in tunnels (ACI 506.1R). Fiber-reinforced shotcrete can also be used as a final or permanent lining for underground structures.

Swimming pools are another application for fiber-reinforced shotcrete. Fiber-reinforced shotcrete is especially suitable for pools and skate parks with many curves, as it is shot against excavated soil, eliminating the cost of forms and steel installation. The flexibility of placement that shotcrete affords allows every pool owner to have a uniquely shaped pool. This material has also become the material of choice for an increasing number of architectural and landscaping applications. Fiber-reinforced shotcrete can often be completed faster and more economically than poured concrete with steel bars or mesh because of the reduced time associated with installation, inspection, and construction of steel shapes and formwork.

Fiber-reinforced shotcrete is an ideal technique when repair and restoration are being contemplated, especially when access is an issue. From canals and pools to retaining walls and hydraulic structures, the opportunities are countless. When fibers are used in repair shotcrete, the need for cutting and placing steel reinforcement for the repair areas is eliminated and the job can be done faster and at less cost. ACI 506.1R has detailed recommendations on fiber-reinforced shotcrete. This document recommends using ASTM C1609/C1609M (FRC beams) or ASTM C1550 (FRC round panels) to determine the performance of fiber-reinforced shotcrete for design and specification purposes. Using the stress block approach for equivalent bending moment, described in Chapter 4, the required fiber dosage for the applied loads and moment can be determined.

Fig. 5.6a—Canal repair using synthetic macrofiber shotcrete in Phoenix, AZ.

Fig. 5.6b—Rock stabilization using steel fiber-reinforced shotcrete.

For mining and tunneling applications, flexural toughness (energy absorption) of fiber-reinforced shotcrete becomes a determining factor for design. In this case, ASTM C1550 is often used to characterize round determinate panels. The required toughness values may vary for specific applications or the given conditions. For example, Australia Office of Mine Safety and Health requires 280, 360, and 450 joules of energy absorption for low-, moderate-, and high-level ground support conditions, respectively (AuSS 2010). The actual requirement for the toughness value is determined for the specific project based on the ground support load levels. Another test method applicable to shotcrete is by using indeterminate square panels according to BS EN 14488:2006 for testing sprayed concrete. Applications of fiber-reinforced shotcrete are shown in Fig. 5.6a and 5.6b.

5.7—Crack control and durability

In many areas, the durability of concrete can be significantly improved by the use of fiber reinforcement (ACI 544.5R). Examples include plastic and restrained shrinkage cracking, which are primary problems that occur in concrete structures with a relatively large surface area such as walls, bridge decks, slabs, and overlays. These applications are susceptible to rapid changes in temperature and humidity, resulting in high water evaporation and high potential for shrinkage cracking. Fiber reinforcement has also been shown to improve the resistance of concrete in exposure to freezing-and-thawing cycles (Balaguru and Ramakrishnan 1986). Using macrofibers in concrete alters the crack widths and spacing that can positively affect the long-term durability.

Thin bridge deck overlays, marine and environmental structures, and tunnel linings are some of the applications where fiber reinforcement has successfully been used for improved crack control and enhanced durability (Zollo 1975). Cracks in properly designed fiber-reinforced concrete are typically much thinner than those in concrete reinforced with bars. Therefore, the rate of ingress for water and chemicals into concrete becomes much slower, resulting in a longer life span. Moreover, there exists a lot of research and practical experience showing significant reduction in crack width in environmental structures using hybrid reinforcement (bars plus fibers).

For concrete structures retaining water or exposed to external water, cracking is a major cause for reduction in serviceability due to the corrosion of steel reinforcement. In particular, cracking has a significant effect on the durability in an environment with frequent freezing-and-thawing cycles. To ensure proper serviceability, cracking should be examined so that the flexural crack width is not greater than the allowable crack width. ACI 224R limits the allowable crack width to 0.012 in. (0.3 mm) for concrete structures exposed to soil. This value may vary for different applications in various environments. Serviceability limit state design has been discussed in detail for segmental tunnel lining by Bakhshi and Nasri (2015) using both fiber reinforcement and conventional reinforcement. Model Code 2010 (*fib* 2013), CNR-DT 204/2006 (National Research Council 2007), RILEM TC 162-TDF (2003), and DAfStb (2012) are among available references to calculate crack width in concrete sections reinforced by fibers without conventional reinforcement.

CHAPTER 6—CONSTRUCTION PRACTICES

Details on specifying, proportioning, mixing, placing, and finishing FRC have been discussed in ACI 544.3R. A summary of these topics is briefly presented herein as a quick guide for engineers who will be specifying FRC.

6.1—Mixture design recommendations for FRC

In many cases, no changes are necessary to conventional concrete mixture design when fibers are added at low to moderate dosages—that is, up to approximately 30 lb/yd^3 (18 kg/m^3) for steel fibers and approximately 4 lb/yd^3 (2.4 kg/m^3) for synthetic macrofibers. At higher dosages and depending on the fiber type, some adjustments to the mixture design become necessary. This includes adding or increasing the amount of water-reducing admixture (plasticizer) to maintain workability and slump without changing the water-cement ratio (w/c). At much higher dosages, an increase in the paste volume (cementitious materials) and using more fine aggregates can ensure proper accommodation and dispersion of the fibers in the concrete mixture.

6.2—Workability of FRC

Fibers change the rheology of the concrete, which can result in an apparent slump loss. The energy required to consolidate and place fresh FRC, however, is no greater than for fresh plain concrete. An FRC mixture, in general, looks more cohesive than plain concrete. At moderate to high dosages of fibers, the use of plasticizing admixtures (typically mid-range or high-range water reducers) may become necessary to maintain the desired slump for placement. Mechanical vibration can be helpful to properly consolidate fresh FRC. Mixtures that contain fibers at elevated dosages may require higher paste volumes to support proper placing of FRC. Therefore, mixtures such as self-consolidating concrete may be used as a practical solution for placing FRC.

In general, a good pumpable mixture can accommodate low to moderate dosages of fibers with little to no adjustments. Often in the field, because FRC looks different and more cohesive, users may want to add water to make the concrete flow better. This can be detrimental, as too much water will cause a mixture to segregate, block the pump hose, and result in lower strength values. When discharging an FRC mixture into a hopper assembly on a pump truck, the chute should be raised 12 to 18 in. (300 to 450 mm) above the grate (if a grate is present) on the pump to allow the fibers to pass through the grate. A working vibrator on a grate will also improve the FRC's ability to pass through the grate. Round rods will ease the passage of fresh FRC through the grate compared to square rods that may prevent the fibers to pass through.

6.3—Adding and mixing fibers

The addition of fibers to a concrete mixture may or may not require special equipment, depending on the type and dosages of fibers. Devices such as conveyor belts, chutes, loss-in weight dispensers, blowers, and pneumatic tubes can be used to add fibers to the mixer on the job site or at the central batching plant. Synthetic fibers (micro and macro) are relatively light (specific gravity of 0.9) and are typically provided in form of 0.5 to 5 lb (0.22 to 2.23 kg) bags. The fiber bags can be added to the central mixer or the mixer truck either manually or with a dispenser. Steel fibers are relatively heavy (specific gravity of 7.8) and typically come in the form of 50 to 100 lb (20 to 45 kg) bags. Manual addition of these fibers is not easy; therefore, using a conveyer belt or other forms of dispensing systems is recommended. Typical addition of steel and synthetic macrofibers is shown in Fig. 6.3.

For optimized performance, fibers should be dispersed uniformly throughout the concrete. Reducing the batch size or increasing the mixing time may become necessary to achieve a uniform dispersion. It is recommended to add the fibers in a continuous manner. A mixing speed of 10 to 12 rpm is typically used for the rate of addition in trucks. A minimum of 40 revolutions (4 to 5 minutes) after all the fibers are added is recommended for proper mixing and dispersion of fibers in trucks. In the case of mixing in a central mixer, mixing time and revolution rate is performed the same way as plain concrete because there is sufficient shear provided to uniformly disperse the fibers. Similar to fresh plain concrete, the air content of fresh FRC should be tested after adding and mixing all constituents and before placement.

All types and sizes of fibers have the potential to ball up in concrete. This phenomenon is usually caused by the addition of fibers into concrete mixtures that are too dry or into mixtures that have low amounts of cement paste to coat the fibers. In these cases, the lack of sufficient paste can cause loss of slump and may lead to nonuniform distribution of the fibers. Loose fibers in an empty drum may also clump together and fibers that are too long or have varying geometries may also cause problems. A test or trial mixing is always recommended to ensure that the mixture will support the fiber type/dosage and that the batching sequence will not cause any problems. Fibers should be added, either to the fully-mixed concrete, or together with aggregates, but never as the first ingredients.

6.4—Placing, consolidation, and finishing FRC

The use of fiber reinforcement does not usually require special placement techniques, as this material lends itself to conventional placing and consolidating methods. If FRC is used in the form of self-consolidating concrete, the need for

Fig. 6.3—Synthetic and steel macrofibers being added to the mixer truck.

Fig. 6.4—FRC can be finished with similar tools used for unreinforced concrete.

vibration is eliminated. To achieve good surface finish with FRC, proper practices should be implemented, including suitable selection of materials, mixture proportioning, mixing, placing, consolidation, and curing. For floors, either a broom finish or trowel finish can be used, and proper timing is the key to obtaining a desired finished surface. When a broom finish is required, ensure that the equipment used to apply the broom finish is maintained in a clean state and the angle of the broom is low with all passes being made in the same direction. The timing of floating and troweling operations is critical to achieve optimum finishing characteristics; therefore, weather conditions should be considered. To consolidate fresh FRC and bring sufficient mortar or paste to the surface to enhance finishing, laser screed, razor back, or vibrating beam machines can be used. The surface mortar produced as a result of compacting the concrete and the initial power floating is usually sufficient to cover most surface fibers. High-quality finishes have been achieved by following the laser screed with a vibrating highway float before troweling. A finishing trial or mockup prior to placement may be necessary to assist the contractor in gaining experience and obtaining a desired surface appearance. Typical finishing methods for fresh FRC are shown in Fig. 6.4.

Synthetic macrofibers do not rust; however, steel fibers that appear on the surface have the potential to rust over time for concrete exposed to an open environment. Corrosion spots that appear on the surface may affect the aesthetics, but will not affect the integrity or performance of the concrete. Good workmanship, the use of suppressive layers such as dry-shakes, or both, would limit or eliminate such rust spots. Using stainless steel or galvanized steel fibers is another option for eliminating rusting in the exposed fibers. More information regarding the placement and finishing FRC slabs is found in ACI 544.3R.

6.5—Quality control for FRC

Depending on the application and the familiarity of the concrete producer and contractor with FRC, some checks have to be made at a reasonable frequency. The quality control system should include both material control and process control. Material control primarily focuses on controlling the material properties of the delivered product. Continuous testing of post-crack residual strength would be a suitable option for this approach. Typically, a set of beam specimens per certain volume of FRC has to be cast and tested according to ASTM C1609/C1609M or BS EN 14651:2005. For fiber-reinforced shotcrete, round panels are often used for testing in accordance with ASTM C1550 or BS EN 14488:2006. A process control-based approach, however, would focus on controlling all steps when making FRC, rather than testing only the outcome or the final product. Once the residual strength has been determined (initial testing), providing that neither concrete composition, fiber type, or dosage are changed, control of fiber content and distribution will ensure the required performance. Testing post-crack residual strength would, of course, still be essential, but the frequency could be reduced if there is confidence in the reliability of the process.

As a means of quality control right before placement, washout tests could be performed on fresh FRC. In CSA A23.2-16C, samples of fresh FRC are taken from each mixer truck (two to three samples using the air-meter container or a bucket) and fibers are separated from the fresh concrete using a washout technique. For steel fibers, a vibrating magnetic device is used for separating the fibers from fresh FRC. For synthetic macrofibers, the fresh concrete is washed out in a sieve box and the fibers are then collected. These fibers are cleaned, dried, and weighed, and the dosage (in lb/yd^3 [kg/m^3]) is calculated and compared with the specified amount. A similar process can be done for precast units with periodic sampling of the fresh FRC. A reasonable tolerance should be used as a quality control measure for accepting or rejecting the FRC mixture. As an alternative, the specifier may also rely on the batching ticket generated by the concrete producer, based on the measured weight of fibers, for quality control.

6.6—Contraction (control) joints

Saw-cutting control joints for slabs reinforced with fibers can be successfully done. New, clean saw blades are recommended. The saw-cutting can be done shortly after final set, but timing of the sawing is critical so as not to pull up the fibers. If fibers are pulled up, the saw-cutting should be delayed until no fibers are pulled during the process. To ensure that the control joints are activated and to prevent parallel cracking for higher dosages of fibers, the saw-cut depth should be one-third the slab thickness. Otherwise, the depth of saw-cutting and filling of the contraction joints should follow the recommendations found in ACI 302.1R. When fibers are used at higher dosages, in conjunction with low-shrinkage concrete, or both, the spacing of control joints may be increased. Proper timing should be implemented for saw-cutting control joints with extended spacing. More information regarding the saw-cutting of control joints in FRC slabs can be found in ACI 544.3R.

Table 6.7—Summary of fiber reinforcement tests and parameters

	Reinforcement purpose	
	Shrinkage/temperature crack control	Post-crack tensile/flexural capacity
Fiber type	Synthetic microfiber Steel and synthetic macrofiber	Steel and synthetic macrofiber
Test method	ASTM C1579 or ASTM C1581/C1581M*	ASTM C1609/C1609M or ASTM C1550†
Test/spec parameter	Percent in crack width reduction	Flexural residual strength or toughness

*Prescriptive (dosage-based) language may be used instead.

†Equivalent BS tests are EN 14651:2005 and EN 14488:2006.

6.7—Specifying FRC

ASTM C1116/C1116M is the standard specification for FRC and provides four types of FRC with steel, glass, synthetic, and natural fibers. This guide provides detailed information and guidance for testing, specifying, purchasing, and using fibers. Physical and chemical long-term performance of fibers should be considered for any fiber product for specific applications. The specification for FRC may be prescriptive or performance-based, depending on the application. For crack control against plastic and drying shrinkage and thermal stresses, prescriptive specifications are often used in which the type and dosage of fibers are specified, along with concrete properties such as flexural strength and shrinkage of concrete. If the purpose of fiber reinforcement is to provide post-crack flexural and tensile capacity to a concrete section, using performance-based language is necessary. This is summarized in Table 6.7. For more information on specifying FRC, refer to ACI 544.3R.

CHAPTER 7—REFERENCES

Committee documents are listed first by document number and year of publication followed by authored documents listed alphabetically.

American Concrete Institute

ACI 223R-10—Guide for the Use of Shrinkage-Compensating Concrete

ACI 224R-01(08)—Control of Cracking in Concrete Structures

ACI 302.1R-15—Guide to Concrete Floor and Slab Construction

ACI 360R-10—Guide to Design of Slabs-on-Ground

ACI 318-14—Building Code Requirements for Structural Concrete and Commentary

ACI 506.1R-08—Guide to Fiber-Reinforced Shotcrete

ACI 544.2R-89(09)—Measurement of Properties of Fiber Reinforced Concrete

ACI 544.3R-08—Guide for Specifying, Proportioning, and Production of Fiber-Reinforced Concrete

ACI 544.5R-10—Report on the Physical Properties and Durability of Fiber-Reinforced Concrete

ACI 544.6R-15—Report on Design and Construction of Steel Fiber-Reinforced Concrete Elevated Slabs

ACI 544.7R-16—Report on Design and Construction of Fiber-Reinforced Precast Concrete Tunnel Segments

ACI 544.8R-16—Report on Indirect Method to Obtain Stress-Strain Response of Fiber-Reinforced Concrete (FRC)

SP-44—Fiber Reinforced Concrete

SP-81—Fiber Reinforced Concrete—International Symposium

SP-105—Fiber Reinforced Concrete—Properties and Applications

ASTM International

ASTM A820/A820M-16—Standard Specification for Steel Fibers for Fiber-Reinforced Concrete

ASTM C1116/C1116M-10(2015)—Standard Specification for Fiber-Reinforced Concrete

ASTM C78/C78M-16—Standard Test Method for Flexural Strength of Concrete (Using Simple Beam with Third-Point Loading)

ASTM C1550-12—Standard Test Method for Flexural Toughness of Fiber-Reinforced Concrete (Using Centrally Loaded Round Panel)

ASTM C1579-13—Standard Test Method for Evaluating Plastic Shrinkage Cracking of Restrained Fiber Reinforced Concrete (Using a Steel Form Insert)

ASTM C1581/C1581M-16—Standard Test Method for Determining Age at Cracking and Induced Tensile Stress Characteristics of Mortar and Concrete under Restrained Shrinkage.

ASTM C1609/C1609M-12—Standard Test Method for Flexural Performance of Fiber-Reinforced Concrete (Using Beam with Three-Point Loading)

ASTM D7508/D7508M-10(2015)—Specification for Polyolefin Chopped Strands for Use in Concrete

British Standards Institution

BS EN 14651:2005—Test Method for Metallic Fibre Concrete – Measuring the Flexural Tensile Strength (Limit of Proportionality (LOP), Residual)

BS EN 14488:2006—Testing sprayed concrete – Determination of Energy Absorption Capacity of Fibre Reinforced Slab Specimens

CSA Group

CSA A23.2-16C:2009—Standard Test Method for Determination of Steel or Synthetic Fiber Content in Plastic Concrete

Steel Deck Institute

ANSI/SDI-C1.0:2014—Standard for Composite Steel Floor Deck

Authored references

Altoubat, S.; Yazdanbakhsh, A.; and Rieder, K. A., 2009, "Shear Behavior of Macro-Synthetic Fiber-Reinforced Concrete Beams without Stirrups," *ACI Materials Journal*, V. 106, No. 4, July-Aug., pp. 381-389.

Altoubat, S.; Ousmane, H.; and Barakat, S., 2016, "Experimental Study of In-Plane Shear Behavior of Fiber-Reinforced Concrete Composite Slabs," *Journal of Structural Engineering*, V. 142, No. 3, Mar., p. 04015156 doi: 10.1061/(ASCE)ST.1943-541X.0001413

AuSS, 2010, *Shotcreting in Australia: Recommended Practice*, second edition, Concrete Institute of Australia and The Australian Concrete Society, Sydney, Australia, 84 pp.

Balaguru, P. N., and Ramakrishnan, V., 1986, "Freeze-Thaw Durability of Fiber Reinforced Concrete," *ACI Journal Proceedings*, V. 83, No. 3, May-June, pp. 374-382.

Bakhshi, M., and Nasri, V., 2015, "Design of Segmental Tunnel Linings for Serviceability Limit State," ITA WTC 2015 Congress and 41st General Assembly, Dubrovnik, Croatia.

Batson, G.; Jenkins, E.; and Spatney, R., 1972, "Steel Fibers as Shear Reinforcement in Beams," *ACI Journal Proceedings*, V. 69, No. 10, Oct., pp. 640-644.

Barros, J. A. O.; Taheri, M.; and Salehian, H., 2015, "A Model to Simulate the Moment-Rotation and Crack Width of FRC Members Reinforced with Longitudinal Bars," *Engineering Structures*, V. 100, pp. 43-56. doi: 10.1016/j.engstruct.2015.05.036

Bonakdar, A.; Bakhshi, M.; Shekarchi, M.; and Pinto, J., 2005, "Study of Load-Deflection Response and Flexural Toughness Parameters of SFRC with Center Point Loading," *Proceeding of 3rd International Structural Engineering and Construction Conference*," Shunan, Japan, pp. 65-72.

Bonakdar, A.; Babbitt, F.; and Mobasher, M., 2013, "Physical and Mechanical Characterization of Fiber Reinforced Aerated Concrete," *Cement and Concrete Composites*, V. 38, pp. 82-91. doi: 10.1016/j.cemconcomp.2013.03.006

Buratti, N.; Mazzotti, C.; and Savoia, M., 2011, "Post-Cracking Behaviour of Steel and Macro-Synthetic Fibre-Reinforced Concretes," *Construction & Building Materials*, V. 25, No. 5, pp. 2713-2722. doi: 10.1016/j.conbuildmat.2010.12.022

Conforti, A.; Minelli, F.; Tinini, A.; and Plizzari, G. A., 2015, "Influence of Polypropylene Fibre Reinforcement and Width-to-Effective Depth Ratio in Wide-Shallow Beams," *Engineering Structures*, V. 88, pp. 12-21. doi: 10.1016/j.engstruct.2015.01.037

Cunha, V. M. C. F., 2010, "Steel Fibre Reinforced Self-Compacting Concrete: From Micro-Mechanics to Composite Behaviour," PhD thesis, University of Minho, Braga, Portugal, 467 pp.

DAfStb, 2012, "Steel Fibre Reinforced Concrete," German Committee for Reinforced Concrete (DAfStb), Berlin, Germany.

de la Fuente, A.; Pujadas, P.; Blanco, A.; and Aguado, A., 2012, "Experiences in Barcelona with the Use of Fibres in Segmental Linings," *Tunnelling and Underground*

Space Technology, V. 27, No. 1, pp. 60-71. doi: 10.1016/j.tust.2011.07.001

Destrée, X.; Yao, Y.; and Mobasher, B., 2016, "Sequential Cracking and their Opening in Steel Fiber Reinforced Joint Free Concrete Slabs," *Journal of Materials in Civil Engineering*, V. 28, No. 4, p. 04015158 doi: 10.1061/(ASCE)MT.1943-5533.0001377

Dey, V.; Bonakdar, A.; and Mobasher, M., 2014, "Low Velocity Flexural Impact Response of Fiber Reinforced Aerated Concrete," *Cement and Concrete Composites*, V. 49, pp. 100-110. doi: 10.1016/j.cemconcomp.2013.12.006

di Prisco, M.; Plizzari, G. A.; and Vandewalle, L., 2009, "Fibre Reinforced Concrete: New Design Perspectives," *Materials and Structures*, V. 42, No. 9, pp. 1261-1281. doi: 10.1617/s11527-009-9529-4

Dinh, H. H.; Parra-Montesinos, J. P.; and Wight, J. K., 2010, "Shear Behavior of Steel Fiber-Reinforced Concrete Beams without Stirrup Reinforcement," *ACI Structural Journal*, V. 107, No. 5, Sept.-Oct., pp. 597-606.

El-Dieb, A. S., 2009, "Mechanical, Durability and Microstructural Characteristics of Ultra-High-Strength Self-Compacting Concrete Incorporating Steel Fibers," *Materials & Design*, V. 30, No. 10, pp. 4286-4292. doi: 10.1016/j.matdes.2009.04.024

Fanella, D. A., and Naaman, A. E., 1985, "Stress-Strain Properties of Fiber Reinforced Concrete in Compression," *ACI Journal Proceedings*, V. 82, No. 4, July-Aug., pp. 475-483.

Fantilli, A. P.; Mihashi, H.; and Vallini, P., 2009, "Multiple Cracking and Strain Hardening in Fiber-Reinforced Concrete under Uniaxial Tension," *Cement and Concrete Research*, V. 39, No. 12, pp. 1217-1229. doi: 10.1016/j.cemconres.2009.08.020

Fantilli, A. P.; Mihashi, H.; Vallini, P.; and Chiaia, B., 2011a, "Equivalent Confinement in HPFRCC Columns Measured by Triaxial Test," *ACI Materials Journal*, V. 108, No. 2, Mar.-Apr., pp. 159-167.

Fantilli, A. P.; Vallini, P.; and Chiaia, B., 2011b, "Ductility of Fiber-Reinforced Self-Consolidating Concrete under Multi-Axial Compression," *Cement and Concrete Composites*, V. 33, No. 4, pp. 520-527. doi: 10.1016/j.cemconcomp.2011.02.007

fib, 2013, "Model Code 2010," Ernst & Sohn, Berlin, Germany, 434 pp.

Ghalib, M. A., 1980, "Moment Capacity of Steel Fiber Reinforced Small Concrete Slabs," *ACI Journal Proceedings*, V. 77, No. 4, July-Aug., pp. 247-257.

Gopalaratnam, V. S., and Shah, S. P., 1986, "Properties of Steel Fiber Reinforced Concrete Subjected to Impact Loading," *ACI Journal Proceedings*, V. 83, No. 1, Jan.-Feb., pp. 117-126.

Gopalaratnam, V. S., and Shah, S. P., 1987a, "Failure Mechanisms and Fracture of Fiber Reinforced Concrete," *Fiber Reinforced Concrete—Properties and Applications*, SP-105, American Concrete Institute, Farmington Hills, MI, pp. 1-25.

Gopalaratnam, V. S., and Shah, S. P., 1987b, "Tensile Failure of Steel Fiber Reinforced Mortar," *Journal of Engineering Mechanics*, V. 113, No. 5, May, pp. 635-652. doi: 10.1061/(ASCE)0733-9399(1987)113:5(635)

Harrington, D., and Fick, G., 2014, "Guide to Concrete Overlays: Sustainable Solutions for Resurfacing and Rehabilitating Existing Pavements," third edition, American Concrete Pavement Association, Rosemont, IL.

Henager, C. H., and Doherty, T. J., 1976, "Analysis of Reinforced Fibrous Concrete Beams," *Journal of the Structural Division*, V. 12, Jan., pp. 177-188.

Hillerborg, A., 1985, "The Theoretical Basis of a Method to Determine the Fracture Energy GF of Concrete," *Materials and Structures*, V. 18, No. 4, pp. 291-296. doi: 10.1007/BF02472919

Hoff, G. C., 1982, "Selected Bibliography on Fiber-Reinforced Cement and Concrete," Miscellaneous Paper No. C-76-6, Supplements 1-4, U.S. Army Engineer Waterways Experiment Station, Vicksburg, MS.

International Code Council, 2015, "International Building Code," ICC, Washington, DC, 736 pp.

Kopczynski, C., and Whiteley, M., 2016, "High-Rises, High Seismicity: New Materials and Design Approaches," *CTBUH Journal of Structural Engineering*, Issue III, pp. 20-26.

Kim, M. O., and Bordelon, A., 2015, "Determination of Total Fracture Energy for Fiber-Reinforced Concrete," *Fracture Mechanics: Applications in Concrete*, SP-300, C. Gaedicke and A. Bordelon, eds., American Concrete Institute, Farmington Hills, MI. (CD-ROM)

Kwak, O.; Kim, W. S.; and Ki, J., 2002, "Shear Strength of Steel Fiber-Reinforced Concrete Beams without Stirrups," *ACI Structural Journal*, V. 99, No. 4, July-Aug., pp. 530-538.

Lösberg, A., 1978, "Pavement and Slabs-on-Ground with Structurally Active Reinforcement," *ACI Journal Proceedings*, V. 75, No. 12, Dec., pp. 647-657.

Malmberg, B., and Skarendahl, A., 1978, "Method of Studying the Cracking of Fibre Concrete under Restrained Shrinkage," *Testing and Test Methods of Fibre Cement Composites*, RILEM Symposium, Construction Press, Lancaster, PA, pp. 173-179.

Mansur, M. A.; Ong, K. C. G.; and Paramasivam, P., 1986, "Shear Strength of Fibrous Concrete Beams Without Stirrups," *Journal of Structural Engineering*, V. 112, No. 9, pp. 2066-2079. doi: 10.1061/(ASCE)0733-9445(1986)112:9(2066)

Meyerhof, G. G., 1962, "Load-Carrying Capacity of Concrete Pavements," *Journal of the Soil Mechanics and Foundations Division*, June, pp. 89-117.

Miltenberger, M. A., and Attiogbe, E. K., 2002, "Shrinkage-Based Analysis for Control-Joint Spacing in Slabs-on-Ground," *ACI Structural Journal*, V. 99, No. 3, May-June, pp. 352-359.

Minelli, F., and Vecchio, F. J., 2006, "Compression Field Modeling of Fiber-Reinforced Concrete Members under Shear Loading," *ACI Structural Journal*, V. 103, No. 2, Mar.-Apr., pp. 244-252.

Minelli, F.; Tiberti, G.; and Plizzari, G. A., 2011, "Crack Control in RC Elements with Fibre Reinforcement," *Advances in FRC Durability and Field Applications*, SP-280, C.-M. Aldea and M. Ekenel, eds., American Concrete Institute, Farmington Hills, MI, 18 pp.

Minelli, F.; Conforti, A.; Cuenca, E.; and Plizzari, G. A., 2014, "Are Steel Fibres Able to Mitigate or Eliminate Size Effect in Shear?" *Materials and Structures*, V. 47, No. 3, pp. 459-473. doi: 10.1617/s11527-013-0072-y

Mobasher, B., 2011, *Mechanics of Fiber and Textile Reinforced Cement Composites*, CRC press, 480 pp.

Mobasher, B.; Bakhshi, M.; and Barsby, C., 2014, "Back Calculation of Residual Tensile Strength of Regular and High-Performance Fiber Reinforced Concrete From Flexural Tests," *Construction & Building Materials*, V. 70, pp. 243-253. doi: 10.1016/j.conbuildmat.2014.07.037

Mobasher, B.; Bonakdar, A.; and Bakhshi, M., 2015a, "Back-Calculation Procedure for Cyclic Flexural Fracture Tests in Fiber Reinforced Concrete," *Fracture Mechanics Applications in Concrete*, SP-300, American Concrete Institute, Farmington Hills, MI. (CD-ROM)

Mobasher, B.; Yao, Y.; and Soranakom, C., 2015b, "Analytical Solutions for Flexural Design of Hybrid Steel Fiber Reinforced Concrete Beams," *Engineering Structures*, V. 100, pp. 164-177. doi: 10.1016/j.engstruct.2015.06.006

Moccichino, M.; Romualdi, P.; Perruzza, P.; Meda, A.; and Rinaldi, Z., 2006, "Experimental Tests on Tunnel Precast Segmental Lining with Fibre Reinforced Concrete," World Tunnel Congress ITA – AITES, Seoul, South Korea.

Naaman, A. E., 2007, "Deflection Softening and Deflection Hardening FRC Composites: Characterization and Modeling," *Deflection and Stiffness Issues in FRC and Thin Structural Elements*, SP-248, P. Bischoff and R. Malhas, eds., American Concrete Institute, Farmington Hills, MI, pp. 53-66.

Naaman, A. E., and Reinhardt, H. W., eds., 1996, "High Performance Fiber Reinforced Cement Composites," HPFRCC 2, RILEM, No. 31, E&FN Spon, London, UK, 505 pp.

Naaman, A. E., and Shah, S. P., 1976, "Pull-Out Mechanism in Steel Fiber Reinforced Concrete," *Journal of the Structural Division*, V. 102, Aug., pp. 1537-1548.

National Research Council, 2007, "Guidelines for the Design, Construction and Production Control of Fibre Reinforced Concrete Structures," CNR-DT 204/2006, National Research Council, Rome, Italy, 57 pp.

NCPA, 2010, *Best Practices Manual: Onsite Wastewater Systems*, third edition, National Precast Concrete Association, Carmel, IN.

NCPA, 2011, *Best Practices Manual: Storm Water System Management*, National Precast Concrete Association, Carmel, IN.

NCPA, 2012, *Quality Control Manual for Precast And Prestressed Concrete Plants*, ninth edition, National Precast Concrete Association, Carmel, IN.

Olesen, J., 2001, "Fictitious Crack Propagation in Fiber-Reinforced Concrete Beams," *Journal of Engineering Mechanics*, V. 127, No. 3, pp. 272-280. doi: 10.1061/(ASCE)0733-9399(2001)127:3(272)

Parra-Montesinos, G. J., 2006, "Shear Strength of Beams with Deformed Steel Fibers," *Concrete International*, V. 28, No. 11, Nov., pp. 57-66.

Paul, S. L., and Sinnamon, G. K., 1975, "Concrete Tunnel Liners: Structural Testing of Segmented Liners," *Final Report* No. FRA-ORD-75-93, U.S. Department of Transportation, University of Illinois, Urbana, IL, Aug., 170 pp.

Paul, B. K.; Polivka, M.; and Mehta, P. K., 1981, "Properties of Fiber Reinforced Shrinkage-Compensating Concrete," *ACI Journal Proceedings*, V. 78, No. 6, Nov.-Dec., pp. 488-492.

Paultre, P.; Eid, R.; Langlois, Y.; and Lévesque, Y., 2010, "Behavior of Steel Fiber-Reinforced High-Strength Concrete Columns under Uniaxial Compression," *Journal of Structural Engineering*, V. 136, No. 10, pp. 1225-1235. doi: 10.1061/(ASCE)ST.1943-541X.0000211

Plizzari, G. A., and Tiberti, G., 2006, "Steel Fibers as Reinforcement for Precast Tunnel Segments," *Tunnelling and Underground Space Technology*, V. 21, No. 3-4, pp. 438-439. doi: 10.1016/j.tust.2005.12.079

Plizzari, G. A., and Tiberti, G., 2007, "Structural Behaviour of SFRC Tunnel Segments," *Proceedings of the 6th International Conference on Fracture Mechanics of Concrete and Concrete Structures (FraMCos 2007)*, A. Carpinteri, P. Gambarova, G. Ferro, and G. A. Plizzari, eds., Catania, Italy, V. 3, pp. 1577-1584.

RILEM TC 162-TDF, 2003, "Final Recommendation of RILEM 162-TDF: Test and Design Methods for Steel Fibre Reinforced Concrete σ-ε Design Method," *Materials and Structures*, V. 36, No. 262, pp. 560-567.

Romualdi, J. P., and Batson, G. P., 1963, "Behavior of Reinforced Concrete Beams with Closely Spaced Reinforcement," *ACI Journal Proceedings*, V. 60, No. 6, June, pp. 775-790.

Shah, S. P., and Rangan, B. V., 1970, "Effects of Reinforcements on Ductility of Concrete," *Journal of the Structural Division*, V. 96, June, pp. 1167-1184.

Shah, S. P., and Skarendahl, A., eds., 1986, *Steel Fiber Concrete*, Elsevier Applied Science Publishers, London, UK, 520 pp.

Shah, S. P.; Stroeven, P.; Dalhuisen, D.; and Van Stekelenburg, P., 1978, "Complete Stress-Strain Curves for Steel Fibre Reinforced Concrete in Uniaxial Tension and Compression," *Testing and Test Methods of Fibre Cement Composites*, RILEM Symposium, Construction Press, Lancaster, pp. 399-408.

Shoaib, A.; Lubell, A. S.; and Bindiganavile, V. S., 2012, "Shear in Steel Fiber Reinforced Concrete Members without Stirrups," *Structural Engineering Report No. 295*, University of Alberta, Edmonton, AB, Canada, 357 pp.

Shoaib, A.; Lubell, A. S.; and Bindiganavile, V. S., 2014, "Size Effect in Shear for Steel-Fiber-Reinforced Concrete Members without stirrups," *ACI Structural Journal*, V. 111, No. 5, Sept.-Oct., pp. 1081-1090. doi: 10.14359/51686813

Schrader, E. K., 1981, "Impact Resistance and Test Procedure for Concrete," *ACI Journal Proceedings*, V. 78, No. 2, Mar.-Apr., pp. 141-146.

Soranakom, C., and Mobasher, M., 2007, "Closed-Form Solutions for Flexural Response of Fiber-Reinforced Concrete Beams," *Journal of Engineering*

Mechanics, V. 133, No. 8, pp. 933-941. doi: 10.1061/(ASCE)0733-9399(2007)133:8(933)

Soranakom, C., and Mobasher, B., 2009, "Flexural Design of Fiber Reinforced Concrete," *ACI Materials Journal*, V. 106, No. 5, Sept.-Oct., pp. 461-469.

Stang, H., and Olesen, J. F., 1998, "On the Interpretation of Bending Tests on FRC Materials, Fracture Mechanics of Concrete Structures," *Proceedings* FRAMCOS-3, Freiburg, Germany.

Swamy, R. N., and Stavrides, H., 1979, "Influence of Fiber Reinforcement on Restrained Shrinkage and Cracking," *ACI Journal Proceedings*, V. 76, No. 3, Mar., pp. 443-460.

Swamy, R. N.; Mangat, P. S.; and Rao, C. V. S. K., 1974, "The Mechanics of Fiber Reinforcement of Cement Matrices," *Fiber Reinforced Concrete*, SP-44, American Concrete Institute, Farmington Hills, MI, pp. 1-28.

Swamy, R. N.; Al-Ta'an, S. A.; and Ali, S. A. R., 1979, "Steel Fibers for Controlling Cracking and Deflection," *Concrete International*, V. 1, No. 8, Aug., pp. 41-49.

Talboys, L. N., and Lubell, A. S., 2014, "Shear in SFRC Slabs Reinforced with High-Strength Steel," *ACI Structural Journal*, V. 111, No. 6, Nov.-Dec., pp. 1431-1440. doi: 10.14359/51687103

Tiberti, G.; Minelli, F.; Plizzari, G. A.; and Vecchio, F. J., 2014, "Influence of Concrete Strength on Crack Development in SFRC Members," *Cement and Concrete Composites*, V. 45, pp. 176-185. doi: 10.1016/j.cemconcomp.2013.10.004

Tiberti, G.; Plizzari, G. A.; Walraven, J. C.; and Blom, C. B. M., 2008, "Concrete Tunnel Segments with Combined Traditional and Combined Reinforcement," *Tailor Made Concrete Structures*, pp. 199-205.

Vandewalle, L., 2000a, "Test and Design Methods for Steel Fiber Reinforced Concrete – Recommendations for Bending Tests," *Materials and Structures*, V. 33, No. 225, Jan.-Feb., pp. 3-5.

Vandewalle, L., 2000b, "Test and Design Methods for Steel Fiber Reinforced Concrete Recommendations for σ-ε Design Method," *Materials and Structures*, V. 33, No. 226, Mar., pp. 75-81.

Vandewalle, L., 2000c, "Cracking Behavior of Concrete Beams Reinforced with a Combination of Ordinary Reinforcement and Steel Fibers," *Materials and Structures*, V. 33, No. 3, pp. 164-170. doi: 10.1007/BF02479410

Vandewalle, L., 2002, "Design of Steel Fibre Reinforced Concrete Using σ-w Method: Principles and Applications," *Materials and Structures*, V. 35, No. 5, pp. 262-278. doi: 10.1007/BF02482132

Vandewalle, L., 2003, "Test and Design Methods for Steel Fiber Reinforced Concrete – σ-ε Design Method – Final Recommendation," *Materials and Structures*, V. 36, No. 262, Oct., pp. 560-567. doi: 10.1617/14007

Visalvanich, K., and Naaman, A. E., 1983, "Fracture Model for Fiber Reinforced Concrete," *ACI Journal Proceedings*, V. 80, No. 2, Mar.-Apr., pp. 128-138.

Westergaard, H. M., 1923, "On the Design of Slabs on Elastic Foundation with Special Reference to Stresses in Concrete Pavements," *Ingenioren*, V. 12, Copenhagen. (in German).

Westergaard, H. M., 1925, "Theory of Stresses in Road Slabs," *Proceedings*, 4th Annual Meeting, Highway Research Board, Washington, DC.

Westergaard, H. M., 1926, "Stresses in Concrete Pavements Computed by Theoretical Analysis," *Public Roads*, V. 7, No. 2, Apr., pp. 25-35.

Williamson, G. R., 1974, "The Effect of Steel Fibers on the Compressive Strength of Concrete," *Fiber Reinforced Concrete*, SP-44, American Concrete Institute, Farmington Hills, MI, pp. 195-207.

Yazdanbakhsh, A.; Altoubat, S.; and Rieder, K. A., 2015, "Analytical Study on Shear Strength of Macro Synthetic Fiber Reinforced Concrete Beams," *Engineering Structures*, V. 100, pp. 622-632. doi: 10.1016/j.engstruct.2015.06.034

Zollo, R. F., 1975, "Wire Fiber Reinforced Concrete Overlays for Orthotropic Bridge Deck Type Loadings," *ACI Journal Proceedings*, V. 72, No. 10, Oct., pp. 576-582.

APPENDIX—SOLVED EXAMPLE PROBLEMS FOR SECTION 4.9—PARAMETRIC BASED DESIGN FOR FRC

The sample problems are constructed under three different cases:

Case A: The cross section and length of the beam and the residual strength of the material are specified; the maximum allowable load is required for the given materials and geometry.

Case B: The cross section, length of the beam, and the loading condition (moment demand) are known; the level of residual strength is required.

Case C: The section details of the slab are known; replacement of steel in the slab by fiber per unit width is required.

Note: Fibers should not be used as the sole reinforcement of simply-supported beams. These examples are presented only for educational purposes to help the designer understand and implement parametric FRC design in 4.9. Fibers, however, can be used in slabs-on-ground and other applications with continuous support or with higher degrees of redundancy. Fibers can also be used in conjunction with reinforcing bars in simply-supported beams.

Case A: Calculation of the moment capacity of a given section

The aim of this section is to use the simplified ultimate strength approach and compare the parametric design of FRC with the solutions obtained from ACI 544.8R to illustrate the process of obtaining moment capacity for a section and compute the allowable service load.

Problem statement: Compute the maximum allowable load on a simply supported beam with a span of L = 4 ft (1.21 m) and a rectangular section 6 x 12 in. (152 x 305 mm). FRC concrete has f_c' = 6000 psi (41.4 MPa). Design for a material with $f_{eq,3}$ = 350 psi (2.4 MPa). Assume a concrete density as ρ_c = 150 lb/ft^3 (2402.7 kg/m^3) and compute the factored moment by assuming ϕ = 1 (ϕ is strength reduction factor that is less than 1 in accordance to ACI 318-14 Section 10.5.1).

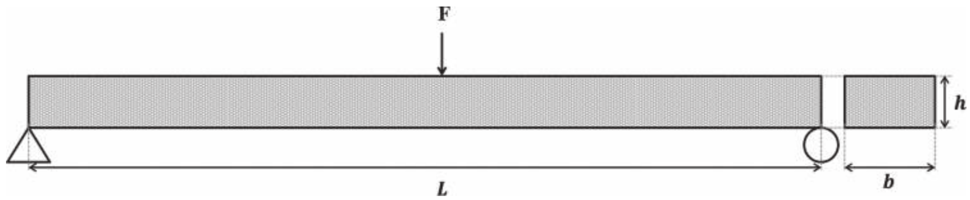

Fig. A.1a—Simply supported beam with center-point loading.

For illustration of the calculation and comparison, Fig. A.1a shows a schematic view of simply supported beam under center-point loading.

Step 1: Define geometric and material parameters

L = 4 ft (1.21 m)

b = 12 in. (0.3 m)

h = 6 in. (0.15 m)

$\phi = 1$

f_c' = 6 ksi (41 MPa)

Assume $\gamma = 1$, thus, $E_c = E$; also, $f_t' = 6.7\sqrt{f_c'}$

$E = 57{,}000\sqrt{f_c'} = 57{,}000\sqrt{6000} = 4.41 \times 10^6$ psi (30 GPa)

$\sigma_{cr} = 6.7\sqrt{f_c'} = 6.7\sqrt{6000} = 518.9$ psi (3.5 MPa)

$$\varepsilon_{cr} = \frac{\sigma_{cr}}{E} = \frac{518.9\text{ psi}}{4.41\times10^6\text{ psi}} = 1.17\times10^{-4}$$

β_{tu} is the normalized ultimate tensile strain in the section and because it is assumed that the section will maintain its residual tensile strength. This value is expected to be imposed as a large number. In this example, it is considered to be equal to 50—that is, $\beta_{tu} = \varepsilon_{tu}/\varepsilon_{cr} = 50$. Therefore, maximum tensile strain allowed is $\varepsilon_{tu} = 0.0055$ or 0.55 percent. The ratio of compressive strength to tensile strength, ω, is obtained as (according to Eq. (4.9e))

$$\omega = \frac{f_c'}{f_t'} \approx \frac{0.85 f_c'}{\varepsilon_{cr}\gamma E} \approx \frac{0.85(6000\text{ psi})}{(1.17\times10^{-4})(1)(4.41\times10^6\text{ psi})} = 9.86$$

Step 2: Calculate demand moment

For a simply supported beam, the maximum moment is at the center of the beam. The demand is computed as summation of moment due to the beam distributed self-weight and the applied concentrated load. In this example, for simplicity, no load factors are applied.

$$M_u = M_{DL} + M_F = \frac{wL^2}{8} + \frac{PL}{4}$$

where M_{DL} is moment due to service dead weight, and M_F is the moment due to point load F:

$$w = \rho bh = (150\text{ lb/ft}^3)\frac{(6\text{ in.})(12\text{ in.})}{144\text{ in.}^2/\text{ft}^2} = 75\text{ lb/ft (1.09 kN/m)}$$

$$M_{DL} = \frac{wL^2}{8} = \frac{(75\text{ lb/ft})(4\text{ ft})^2}{8} = 150\text{ lb-ft (0.203 kN-m)}$$

$$\phi M_n = M_u = 150\text{ lb}\times\frac{1\text{ kip}}{1000\text{ lb}} + \frac{F(4\text{ ft})}{4}\text{ kip-ft}$$

$$\left(0.203 + \frac{F(1.21\text{ m})}{4}\text{ kN-m}\right)$$

Step 3: Calculate cracking moment

Cracking moment is given by:

$$M_{cr} = \frac{1}{6}\sigma_{cr}bh^2$$

$$= \frac{1}{6}(518.9\text{ psi})(12\text{ in.})(6\text{ in.})^2 \times \frac{1\text{ ft}}{12\text{ in.}} \times \frac{1\text{ kip}}{1000\text{ lb}}$$

$$= 3.1\text{ kip-ft (4.2 kN-m)}$$

Step 4: Determine post-crack tensile strength (ACI 544.8R)

Use the formula for plain FRC in accordance with Eq. (4.9g):

$$M_n = \left[\frac{6 f_{eq,3}\sqrt{f_c'}}{\xi(f_{eq,3} + 2.54 f_c')}\right] M_{cr}$$

$\xi = 15.8$ for in.-lb units; $\xi = 1.32$ for SI units

$$= \left[\frac{6(350\text{ psi})\sqrt{6000}}{15.8(350\text{ psi}) + (2.54)(6000)}\right] \times 3.1\text{ kip-ft}$$

$$= 2.056\text{ kip-ft}$$

$\phi M_n = M_u = (0.15 + F)$ kip-ft = 2.056 kip-ft

F = 1.9 kip

In SI units, the equation would yield the same results:

$$M_n = \left[\frac{6(2.41\text{ MPa})\sqrt{41.36}}{1.32(2.41\text{ MPa}) + (2.54)(41.36)}\right] \times 4.2\text{ kN-m}$$

$$= 2.78\text{ kN-m}$$

$\phi M_n = M_u = (0.203 + [F(1.21\text{ m})/4])$ kN-m = 2.78 kN-m

F = 8.52 kN

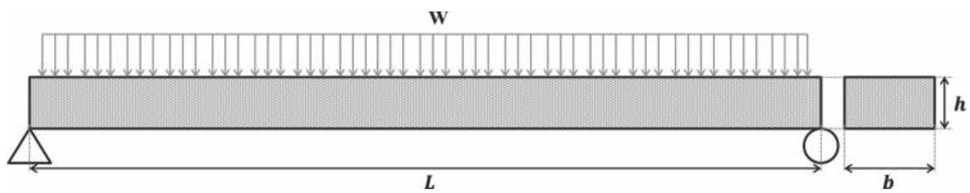

Fig. A.1b—Example beam, dimensions and loading.

Case B: Calculation of μ based on parametric-based design for FRC (ACI 544.8R)

The aim of this section is to use the simplified ultimate strength approach and compare the parametric design of FRC with the solutions obtained from ACI 544.8R to illustrate the process of obtaining μ for a given service load. A simply supported beam with a span of L = 3 ft (0.91 m) and a rectangular section 6 x 5 in. (152.4 x 127 mm) is used as the base design. The service distributed load of LL = 90 lb/ft (1.31 kN/m) in addition to self-weight are used. FRC concrete has tensile cracking strength of σ_{cr} = 328 psi (2.3 MPa) and f_c' = 3000 psi (20.68 MPa). Concrete density of ρ_c = 150 lb/ft^3 (2400 kg/m^3) and ϕ = 1 is used. It is assumed that the serviceability limit is equal to 30—that is, $\beta_{tu} = \varepsilon_{tu}/\varepsilon_{cr} = 30$.

a) Compute the required material parameter μ to carry the load in the post-peak region

b) Solve Case A for three depths of 5, 7, and 9 in. (127, 178, and 230 mm)

c) Solve Case A for a cantilever beam of L = 3 ft (0.91 m)

For illustration of the calculation and comparison, only Case B is addressed in this example. The results of the other cases are presented at the end of this example. Figure A.1b shows a schematic side view of simply supported beams under a uniformly distributed loading.

Step 1: Define geometric and material parameters

L = 3 ft (0.91 m)

b = 6 in. (0.152 m)

d = 5 in. (0.127 m)

ϕ = 1

f_c' = 3000 psi (20.68 MPa)

σ_{cr} = 328 psi (2.3 MPa)

also assume γ = 1, thus $E_c = E$.

$$E = 57{,}000\sqrt{f_c'} = 57{,}000\sqrt{3000} = 3.12 \times 10^6 \text{ psi (21.5 GPa)}$$

$$\varepsilon_{cr} = \frac{\sigma_{cr}}{E} = \frac{328 \text{ psi}}{3.12\times10^6 \text{ psi}} = 1.1\times10^{-4}$$

In this example, it is assumed that the serviceability limit is equal to 30—that is, $\beta_{tu} = \varepsilon_{tu}/\varepsilon_{cr} = 30$. Therefore, maximum tensile strain allowed is ε_{tu} = 0.0033, or 0.33 percent. The ratio of allowable compressive strength to tensile strength, ω, is obtained as:

$$\omega = \frac{0.85 f_c'}{\varepsilon_{cr}\gamma E} = \frac{0.85\times3000 \text{ psi}}{0.00011\times1\times3.12\times10^6 \text{ psi}} = 7.42$$

Step 2: Calculate demand moment

The design is based on a distributed live load of LL = 90 lb/ft (1.31 kN/m) and dead load due to self-weight assuming ρ_c = 150 lb/ft^3 (2402.7 kg/m^3) is calculated as:

$$DL = \frac{(6 \text{ in.})(5 \text{ in.})}{144 \text{ in.}^2/\text{ft}^2}\times150 \text{ lb/ft}^3 = 31.25 \text{ lb/ft (0.45 kN/m)}$$

$w = 1.2 \times DL + 1.6 \times LL$ = (1.2 × 31.25 lb/ft) + (1.6 × 90 lb/ft) = 181.5 lb/ft (2.64 kN/m)

For a simply supported beam the maximum moment is at the center of the beam:

$$M_u = \frac{wl^2}{8} = \frac{181.5 \text{ lb/ft} \times (3 \text{ ft})^2}{8} = 204.2 \text{ lb-ft (0.276 kN-m)}$$

Step 3: Calculate cracking moment

Cracking moment is given by:

$$M_{cr} = \frac{1}{6}\sigma_{cr}bh^2 = \frac{1}{6}\times328 \text{ psi}\times(6 \text{ in.})\times(5 \text{ in.})^2$$
$$= 683.33 \text{ lb-ft (0.926 kN-m)}$$

$$m_\infty = \frac{M_u}{M_{cr}} = \frac{204.2 \text{ lb-ft}}{683.33 \text{ lb-ft}} = 0.298$$

Step 4: Determine post-crack tensile strength (using ACI 544.8R)

Taking the ultimate state formula, for plain FRC, in consideration to Eq. (4.9i):

$$\mu = \frac{2m_\infty\sqrt{f_c'}}{6\sqrt{f_c'} - m_\infty\xi}$$

$$\mu = \frac{2(0.298)\sqrt{3000 \text{ psi}}}{6\sqrt{3000 \text{ psi}} - (0.298)15.8} = 0.10$$

The value of μ given by Eq. (4.9i) can be verified in the next section using the entire moment curvature response by the ACI 544.8R Excel worksheet (Mobasher et. al. 2015a).

Alternatively, if the problem is approached from a serviceability criteria and limits the magnitude of the bending moment to strain levels dictated by $\beta_{tu} = \varepsilon_{tu}/\varepsilon_{cr} = 30$ or ε_{tu} = 0.0033, calculate the corresponding compression strain λ_{cu}, which is obtained using procedures presented in Soranakom and Mobasher (2009) as $\lambda_{cu} = \sqrt{2\mu\beta - 2\mu + 1}$. Using a spreadsheet or hand calculation for two values of μ = 0.05 and 0.15 obtain λ_{cu} of 1.97 and 3.11, respectively, that, once used in Eq. (4.9a) and (4.9b), would yield moment values of 0.149 and 0.44. A simple linear interpolation between these

Table A.1a—Dimensions and support conditions for the beam examples

Case	Beam type	Loading type	L, ft (m)	b, in. (m)	h, in. (m)	DL, lb/ft (kN/m)	LL, (lb/ft) (kN/m)	w, (lb/ft) (kN/m)	M_u, lb-ft (kN-m)	μ
1	Simply supported beam	DL	3 (0.91)	6 (0.2)	5 (0.12)	31.25 (0.45)	90 (1.3)	181 (2.64)	204.2 (0.276)	0.10
2		DL	3 (0.91)	6 (0.2)	7 (0.17)	43.75 (0.63)	90 (1.3)	196.5 (2.86)	221.0 (0.30)	0.055
3		DL	3 (0.91)	6 (0.2)	9 (0.22)	56.25 (0.82)	90 (1.3)	211.5 (3.08)	237.9 (0.322)	0.035
4	Cantilever beam	DL	3 (0.91)	6 (0.2)	5 (0.13)	31.25 (0.45)	90 (1.3)	181.5 (2.64)	816.75 (1.10)	0.41
5		DL	3 (0.91)	6 (0.2)	7 (0.17)	43.75 (0.63)	90 (1.3)	196.5 (2.86)	884.25 (1.19)	0.22
6		DL	3 (0.91)	6 (0.2)	9 (0.22)	56.25 (0.82)	90 (1.3)	211.5 (3.08)	951.75 (1.29)	0.145

Notes: DL: distributed load, LL: Live load.
Spreadsheet back-calculation procedure is explained in detail in the validation section of the report, based on ACI 544.8R. Results of all the sections analyzed are shown in Fig. A.1c.

two bounds for a demand moment of 0.298 would yield a value of μ = 0.094, as the required residual strength,

Validation of the results by back-calculation using Excel worksheet based on ACI 544.8R—To compute the stress-strain diagrams from flexural test data, a generalized Excel spreadsheet for inverse analysis is available for simulation of the moment-curvature response as a design tool in Appendix A of ACI 544.8R (Mobasher et al. 2015a). In this approach, the parametric and geometrical values are used to obtain the behavior of the section based on full models of tension and compression to obtain the M-ϕ curve. The steps are as follows:

a) Enter or assume a value of μ in the ACI 544.8R spreadsheet. Input the dimension of the flexural beam sample and the material properties.

b) Inspect the M-ϕ curve and choose the magnitude of the moment in the post-peak region corresponding to the level of serviceability strain at β_{tu} = 30 or 50.

c) Check whether the value of residual moment in the post-peak region corresponds to demand moment. Repeat the process to make sure that your input values satisfy the demand moment needed.

On the same steps, five more beam cross sections of different support conditions and different depths (that is, 5, 7, and 9 in. [125, 175, and 225 mm]) of Cases B and C were analyzed in a similar manner and are summarized in Table A.1a.

Figure A.1c shows the compilation of the results from the use of the ACI 544.8R spreadsheet to compute the required parameter μ for a given demand moment. Note that the compressive and tensile stress-strain responses are shown in Fig. A.1c(a) and (b), which, for a given sample geometry, generate the moment-curvature diagram for the two cases of loading that include the cantilever and simply supported beams. The solution of this case matches the simplified solution within a 10 percent tolerance and the load-deflection of the member can also be extracted from the spreadsheet. The reason for the differences are due to assumptions of limit state that calculates the moment at an extremely large curvature versus the serviceability-based assumptions that compute the moment at levels defined by the numerical example such as ε_{tu} = 0.003, or 0.33 percent. Comparison of the results from parametric based design for FRC and the results from ACI Excel worksheet is presented in Table A.1b. This is shown graphically in Fig. A.1d.

Case C: Calculation of μ for the replacement of reinforcement in a singly reinforced slab (ACI 544.8R)

The aim of this section is to replace the given reinforcement in slab with equivalent amount of fibers using ACI 544.8R formulation to illustrate the process of obtaining μ. All the calculations are made per unit width of the slab.

a) Input material properties:

Concrete compressive strength f_c' = 4000 psi (27.57 MPa)

Steel yield strength f_y = 60 ksi (413.86 MPa)

Thickness h = 5 in. (127 mm)

Depth of reinforcement d = 3.75 in. (95.25 mm)

Reinforcement: 6 x 6 in. (W2.9 x W2.9) welded wire mesh

b) Calculation of material parameters for the normalized response

$$E_c = 57{,}000\sqrt{4000} = 3.60\times10^6 \text{ psi } (24.85\,\text{GPa})$$

$$\sigma_{cr} = 6.7\sqrt{f_c'} = 6.7\sqrt{4000} = 424 \text{ psi}\,(2.98 \text{ MPa})$$

$$\varepsilon_{cr} = \frac{\sigma_{cr}}{E} = \frac{423.74\,\text{psi}}{3.6\times10^6\text{ psi}} = 0.000117$$

$$\omega = \frac{\sigma_{cy}}{\sigma_{cr}} = \frac{0.85f_c'}{6.7\sqrt{f_c'}} = 0.127\sqrt{f_c'} = 0.127\sqrt{4000} = 8.02$$

c) Calculation of the existing moment capacity according to ACI 318.

b = 12 in. (306 mm)

h = 5 in. (127 mm)

$A_{st} = 2(\pi/4)(0.192\text{ in.})^2 = 0.058\text{ in.}^2$ (37.4 mm²) per linear ft

$$a = \frac{A_sf_y}{0.85f_c'b} = \frac{(0.058\,\text{in.}^2)(60\,\text{ksi})}{0.85(4\,\text{ksi})(12\,\text{in.})} = 0.085\,\text{in.}\,(2.15\,\text{mm})$$

$$M_n = A_sf_y\left(d-\frac{a}{2}\right)$$

$$= (0.058\,\text{in.}^2)(60\,\text{ksi})\left(3.75\text{ in.}-\frac{0.085\text{ in.}}{2}\right)\frac{1\,\text{ft}}{12\,\text{in.}}$$

$$= 1.075\,\text{kip-ft}\,(1.45\,\text{kN-m})$$

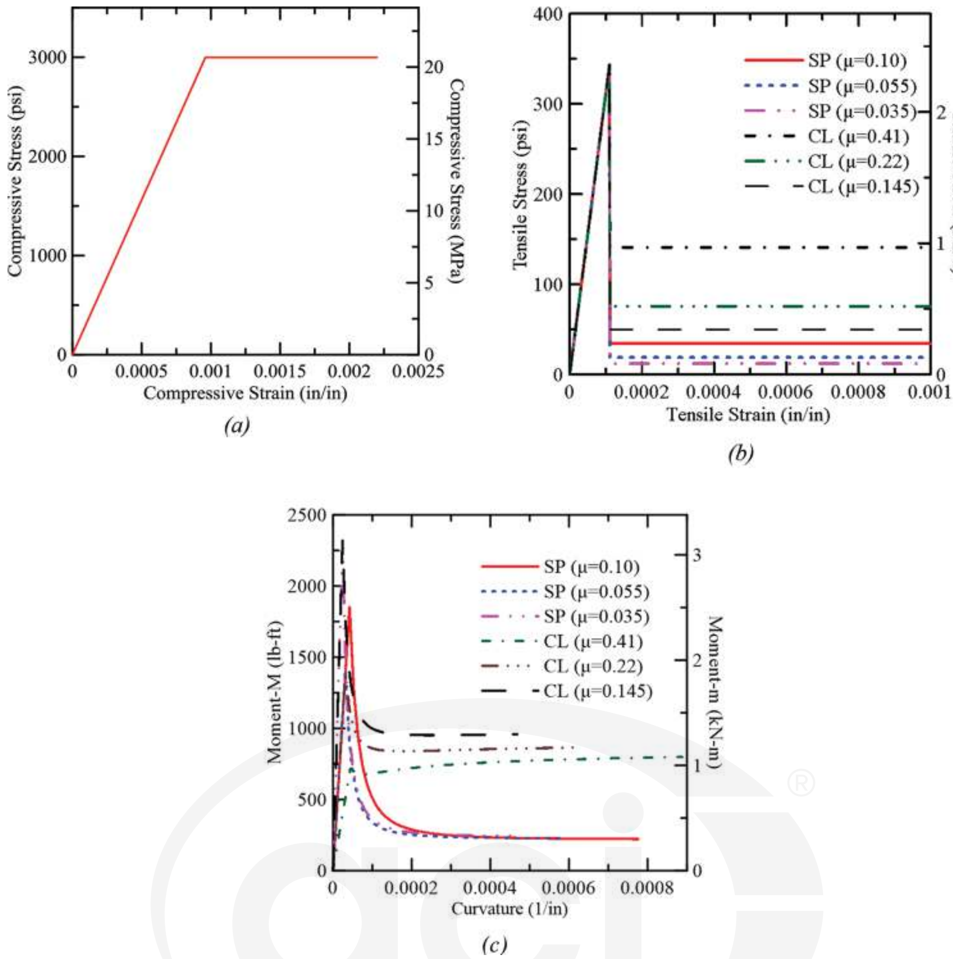

Fig. A.1c—Results from ACI 544.8R spreadsheet calculation (Mobasher et al. 2015a): (a) compression model, stress versus strain; (b) tension model, stress versus strain; and (c) moment-curvature diagram (CL: cantilever beam, SP: simply supported).

Table A.1b—Comparison of results from parametric-based design for FRC and the results from ACI Excel worksheet (ACI 544.8R)

Case study	Required capacity, lb-ft (kN-m)	μ	Moments from spreadsheet inverse analysis calculationm lb-ft (kN-m)	Difference, percent
1	204.2 (0.276)	0.10	221.65 (0.30)	8.22
2	221.0 (0.30)	0.055	227.94 (0.307)	2.71
3	237.9 (0.322)	0.035	244.28 (0.33)	2.86
4	816.75 (1.10)	0.41	797.94 (1.08)	2.32
5	884.25 (1.19)	0.22	864.49 (1.17)	2.26
6	951.75 (1.29)	0.145	958.0 (1.30)	0.73

d) Calculate normalized ultimate moment and σ_{cr} as (this is shown schematically in Fig. A.1e):

$$M_{cr} = \frac{1}{6}\sigma_{cr}bh^2$$
$$= \frac{1}{6}(424\ \text{psi})(12\ \text{in.})(5\ \text{in.})^2\ \frac{1\ \text{kip-ft}}{12{,}000\ \text{lb-in.}}$$
$$= 1.76\ \text{kip-ft}\,(2.39\ \text{kN-m})$$

$$m_\infty = \frac{1.075\ \text{kip-ft}}{1.76\ \text{kip-ft}} = 0.61$$

e) Calculate μ for the required capacity according to ACI 544.8R. The following formulation was used for calculation of μ:

$$\mu = \frac{2m_\infty\sqrt{f_c'}}{6\sqrt{f_c'} - m_\infty\xi}$$

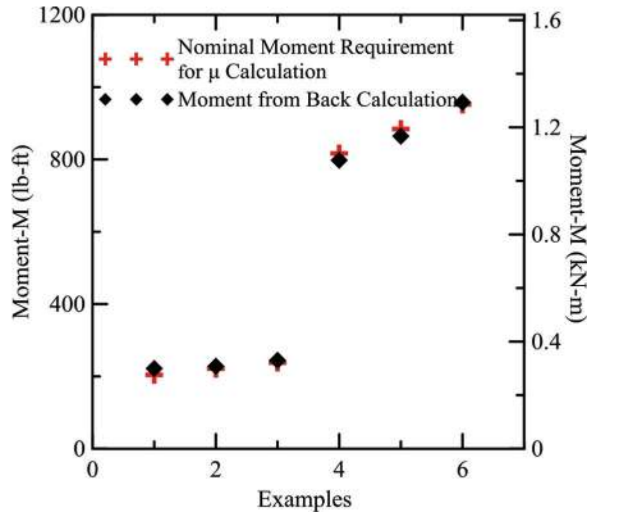

Fig. A.1d—Comparison of ACI 544.8R results versus back calculation results.

where $m_\infty = M_n/M_{cr}$.

$$\mu = \frac{2(0.61)\sqrt{4000\,\text{psi}}}{6\sqrt{4000\,\text{psi}} - 15.8(0.61)} = 0.208$$

$\mu = 0.208$ and $\mu\sigma_{cr} = 0.208 \times 424$ psi = 88.2 psi (0.61 MPa)

At this point, replace the welded wire mesh with a FRC that can provide a residual tensile strength of 88.1 psi (0.607 MPa). To correlate this requirement to flexural data obtained from tests, use the approximations proposed by Mobasher et al. (2014) and use a one-third relationship between the tensile and flexural residual strength; therefore, an approximate flexural strength of 264.3 psi (1.8 MPa) is needed.

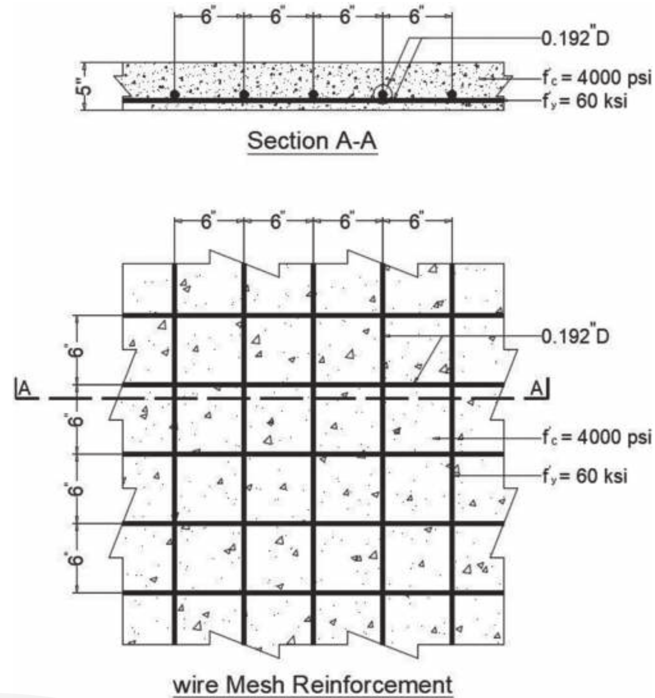

Fig. A.1e—Reinforcement configuration of the 12 in. (300 mm) section taken from the slab.

American Concrete Institute
Always advancing

As ACI begins its second century of advancing concrete knowledge, its original chartered purpose remains “to provide a comradeship in finding the best ways to do concrete work of all kinds and in spreading knowledge.” In keeping with this purpose, ACI supports the following activities:

· Technical committees that produce consensus reports, guides, specifications, and codes.

· Spring and fall conventions to facilitate the work of its committees.

· Educational seminars that disseminate reliable information on concrete.

· Certification programs for personnel employed within the concrete industry.

· Student programs such as scholarships, internships, and competitions.

· Sponsoring and co-sponsoring international conferences and symposia.

· Formal coordination with several international concrete related societies.

· Periodicals: the ACI Structural Journal, Materials Journal, and Concrete International.

Benefits of membership include a subscription to Concrete International and to an ACI Journal. ACI members receive discounts of up to 40% on all ACI products and services, including documents, seminars and convention registration fees.

As a member of ACI, you join thousands of practitioners and professionals worldwide who share a commitment to maintain the highest industry standards for concrete technology, construction, and practices. In addition, ACI chapters provide opportunities for interaction of professionals and practitioners at a local level to discuss and share concrete knowledge and fellowship.

American Concrete Institute
38800 Country Club Drive
Farmington Hills, MI 48331
Phone: +1.248.848.3700
Fax: +1.248.848.3701

www.concrete.org

American Concrete Institute
Always advancing

38800 Country Club Drive
Farmington Hills, MI 48331 USA
+1.248.848.3700
www.concrete.org

The American Concrete Institute (ACI) is a leading authority and resource worldwide for the development and distribution of consensus-based standards and technical resources, educational programs, and certifications for individuals and organizations involved in concrete design, construction, and materials, who share a commitment to pursuing the best use of concrete.

Individuals interested in the activities of ACI are encouraged to explore the ACI website for membership opportunities, committee activities, and a wide variety of concrete resources. As a volunteer member-driven organization, ACI invites partnerships and welcomes all concrete professionals who wish to be part of a respected, connected, social group that provides an opportunity for professional growth, networking and enjoyment.

9 781641 950190